

# Towards Understanding Link Predictor Generalizability Under Distribution Shifts

Jay Revolinsky\*  
Michigan State University  
East Lansing, Michigan, USA  
revolins@msu.edu

Harry Shomer\*  
Michigan State University  
East Lansing, Michigan, USA  
shomerha@msu.edu

Jiliang Tang  
Michigan State University  
East Lansing, Michigan, USA  
tangjili@msu.edu

## Abstract

State-of-the-art link prediction (LP) models demonstrate impressive benchmark results. However, popular benchmark datasets often assume that training, validation, and testing samples are representative of the overall dataset distribution. In real-world situations, this assumption is often incorrect; uncontrolled factors lead new dataset samples to come from a different distribution than training samples. Additionally, the majority of recent work with graph dataset shift focuses on node- and graph-level tasks, largely ignoring link-level tasks. To bridge this gap, we introduce a novel splitting strategy, known as LPShift, which utilizes structural properties to induce a controlled distribution shift. We verify LPShift's effect through empirical evaluation of SOTA LP models on 16 LPShift variants of original dataset splits, with results indicating drastic changes to model performance. Additional experiments demonstrate graph structure has a strong influence on the success of current generalization methods. Source Code Available Here: LPShift

## CCS Concepts

• **Mathematics of computing** → **Graph algorithms**; • **Computing methodologies** → **Ranking**.

## Keywords

Link Prediction, Synthetic Graphs, Distribution Shift, Graph Neural Networks

## ACM Reference Format:

Jay Revolinsky, Harry Shomer, and Jiliang Tang. 2018. Towards Understanding Link Predictor Generalizability Under Distribution Shifts. In *Proceedings of Make sure to enter the correct conference title from your rights confirmation email (Conference acronym 'XX)*. ACM, New York, NY, USA, 23 pages. <https://doi.org/XXXXXX.XXXXXXX>

## 1 Introduction

Link Prediction (LP) is concerned with predicting unseen links (i.e., edges) between two nodes in a graph [32]. The task has a wide variety of applications including: recommender systems, [12], knowledge graph completion [33], protein-interaction [27], and drug

discovery [1]. Traditionally, LP was performed using heuristics that model the pairwise interaction between two nodes [2, 36, 65]. The success of Graph Neural Networks (GNNs) [25] has prompted their usage in LP [24, 60]. However, GNNs are unable to fully-capture representations for node pairs [45, 61]. To combat this problem, recent methods (i.e., GNN4LP) empower GNNs with additional information to capture pairwise interactions between nodes [8, 43, 48, 60] and demonstrate tremendous ability to model LP on real-world datasets [21].

While recent methods have shown promise, current benchmarks [21] typically assume that the training and evaluation data is *drawn from the same structural distribution*. This assumption collapses in real-world scenarios, where the structural feature (i.e., covariate) distribution may shift from training to evaluation. Therefore, it's often necessary for models to generalize to samples whose newly-introduced feature distribution differs from the training dataset [6, 51, 55, 56].

Furthermore, while numerous methods work to account for distribution shifts within graph machine learning [30], there remains little work doing so for LP. Specifically, we observe that **(1) No LP Benchmark Datasets**: Current graph benchmark datasets designed with a quantifiable distribution shift are focused solely on the node and graph tasks [9, 67], *with no datasets available for LP*. **(2) Absence of Foundational Work**: There is limited existing work for distribution shifts relevant to LP [62]. Current methods are primarily focused on detecting and alleviating anomalies within node- and graph-level tasks [6, 15, 18, 23, 30, 46, 52, 53]. Additionally, few methods are designed for aiding LP generalization in any setting [10, 62, 63, 67]. Also, other LP generalization methods which are theorized to improve performance in shifted scenarios remain crucially untested [44, 49].

To tackle these problems, this work proposes the following contributions:

- **Creating Datasets with Meaningful Distribution Shifts.**

LP requires pairwise structural considerations [32, 34]. Additionally, when considering realistic settings [31] or distribution shift [68], GNN4LP models perform poorly relative to models used in graph [50, 57] and node classification [42, 64]. To better understand distribution shifts, we use key structural LP heuristics to split the links into train/validation/test splits via LPShift. By applying LPShift to generate dataset splits, we induce shifts in the underlying distribution of the links, thereby affecting formation [34]. Theoretical justification is provided in Section 4.

- **Benchmarking Current LP Methods.** GNN4LP models demonstrate a strong sensitivity to LPShift when generalizing to the synthetic dataset splits. Despite the existence

\*Both authors contributed equally to this research.

Permission to make digital or hard copies of all or part of this work for personal or classroom use is granted without fee provided that copies are not made or distributed for profit or commercial advantage and that copies bear this notice and the full citation on the first page. Copyrights for components of this work owned by others than the author(s) must be honored. Abstracting with credit is permitted. To copy otherwise, or republish, to post on servers or to redistribute to lists, requires prior specific permission and/or a fee. Request permissions from [permissions@acm.org](mailto:permissions@acm.org).  
Conference acronym 'XX, Woodstock, NY

© 2018 Copyright held by the owner/author(s). Publication rights licensed to ACM.  
ACM ISBN 978-1-4503-XXXX-X/2018/06  
<https://doi.org/XXXXXX.XXXXXXX>

of LP generalization methods, such as FakeEdge [10] and Edge Proposal Sets [44], there remains little work benchmarking link-prediction models under distribution shifts [9, 10, 68]. This lack of benchmarking contributes to a gap in understanding, impeding the capabilities of LP models to generalize. This work quantifies the performance of SOTA LP models under 16 unique LPShift scenarios and provides analysis as a foundation for improving LP model generalization. We further quantify the effects of LP and graph-specific generalization methods, finding that they also struggle to generalize with differing structural shifts.

The remainder of this paper is structured as follows. In Section 2, we provide background on the heuristics, models, and generalization methods used in LP. In Section 3, we detail how the heuristics, theoretical perspectives, and HeART [31] relate to our proposed splitting strategy and formally introduce LPShift. Lastly, in Section 5, we benchmark a selection of LP models and generalization methods on LPShift, followed by analysis to understand the effects of this new strategy.

## 2 Related Work

**LP Heuristics:** Classically, neighborhood heuristics, which measure characteristics between source and target edges, functioned as the primary means of predicting links. These heuristics show limited effectiveness with a relatively-high variability in results, largely due to the complicated irregularity within graph datasets; which only grows worse with larger datasets [32]. Regardless of this, state-of-the-art GNN4LP models have integrated these neighborhood heuristics into neural architectures to elevate link prediction capabilities [8, 48].

For a given heuristic function,  $u$  and  $v$  represent the source and target nodes in a potential link,  $(u, v)$ .  $\mathcal{N}(v)$  is the set of all edges, or neighbors, connected to node  $v$ .  $f(v_{i,i+1}, u)$  is a function that considers all paths of length  $i$  that start at  $v$  and connect to  $u$ . The three tested heuristics are as follows:

*Common Neighbors* [36]: The number of neighbors shared by two nodes  $u$  and  $v$ ,

$$\text{CN}(u, v) = |\mathcal{N}(u) \cap \mathcal{N}(v)|. \quad (1)$$

*Preferential Attachment* [32]: The product of the number of neighbors (i.e., the degree) for nodes  $u$  and  $v$ ,

$$\text{PA}(u, v) = |\mathcal{N}(u)| \times |\mathcal{N}(v)|. \quad (2)$$

*Shortest Path Length* [32]: The path between  $u$  and  $v$  which considers the smallest possible number of nodes, denoted as length  $n$ ,

$$\text{SP}(u, v) = \arg \min_{\Sigma} (\sum_{i=1}^{n-1} f(v_{i,i+1}, u)). \quad (3)$$

**GNNs for Link Prediction (GNN4LP):** LP's current SOTA methods rely on GNNs for a given model's backbone. The most common choice is the Graph Convolutional Network (GCN) [25], integrating a simplified convolution operator to consider a node's multi-hop neighborhood. The final score (i.e., probability) of a link existing considers the representation between both nodes of interest. However, [61] show that such methods aren't suitably expressive for LP, as they ignore vital pairwise information that exists between both

nodes. To account for this, SEAL [60] conditions the message passing on both nodes in the target link by applying a node-labelling trick to the enclosed  $k$ -hop neighborhood. They demonstrate that this can result in a suitably expressive GNN for LP. NBFNet [69] conditions the message passing on a single node in the target link by parameterizing the generalized Bellman-Ford algorithm. In practice, it's been shown that conditional message passing is prohibitively expensive to run on many LP datasets [8]. Instead, recent methods take the standard GNN representations and an additional pairwise encoding into their scoring function for link prediction. For the pairwise encoding, Neo-GNN [58] considers the higher-order overlap between neighborhoods. BUDDY [8] estimates subgraph counts via sketching to infer information surrounding a target link. Neural Common-Neighbors with Completion (NCNC) [48] encodes the enclosed 1-hop neighborhood of both nodes. Lastly, LPFormer [43] adapts a transformer to learn the pairwise information between two nodes.

**Generalization in Link Prediction:** Generalization methods for LP rely on a mix of link and node features in order to improve LP model performance. DropEdge [37] randomly removes edges with increasing probability from the training adjacency matrix, allowing for different views of the graph. Edge Proposal Sets (EPS) [44] considers two models – a filter and rank model. The filter model is used to augment the graph with top- $k$  relevant common neighbors, while the rank method scores the final prediction. [49] built Topological Concentration (TC), which considers the overlap in subgraph features for a given node with each connected neighbor, correlating well with LP performance for individual links. To improve the performance of links with a low TC, a re-weighting strategy applies more emphasis on links with a lower TC. Counter-Factual Link Prediction (CFLP) [63] conditions a pre-trained model with edges that contain information counter to the original adjacency matrix, allowing models to generalize on information not present in a provided dataset.

## 3 Benchmark Dataset Construction

In this section, we explain how LPShift induces a shift in each dataset's structure; clarifying the importance of each structural measure and their application to splitting graph data.

### 3.1 Types of Distribution Shifts

We induce distribution shifts by splitting the links based on key structural properties affecting link formation and thereby LP. We consider three type of metrics: Local structural information, Global structural information, and Preferential Attachment. Recent work by [35] has shown the importance of local and global structural information for LP. Furthermore, due to the scale-free nature of many real-world graphs relates to link formation [5], we also consider Preferential Attachment. A representative metric is then chosen for each of the three types, shown as follows:

**(1) Common Neighbors (CNs):** CNs measure *local structural information* by considering only those nodes connected to the target and source nodes. A real-world case for CNs is whether you share mutual friends with a random person, thus determining if they are your "friend-of-a-friend" [2]. CNs plays a large role in GNN4LP, given

**Algorithm 1** Dataset Splitting Strategy (LPShift)**Require:**

$G$  = Initial Graph,  
 $\Psi(\cdot, \cdot)$  = Heuristic function  
 $i_{train}, i_{valid}$  = Heuristic score thresholds  
 $Train, Valid, Test = \emptyset, \emptyset, \emptyset$

```

1: while edge,  $(u, v)$  not visited in  $G$  do
2:    $\Psi(u, v) = h(u, v)$             $\triangleright$  Score edge with neighborhood
    heuristic
3:   if  $h(u, v) \leq i_{train}$  then            $\triangleright$  Train Split
4:      $Train \leftarrow (u, v)$ 
5:   else if  $h(u, v) > i_{train}$  and  $h(u, v) \leq i_{valid}$  then  $\triangleright$  Valid
    split
6:      $Valid \leftarrow (u, v)$ 
7:   else            $\triangleright h(u, v) > i_{valid}$ , Test Split
8:      $Test \leftarrow (u, v)$ 
9:   end if
10: end while
11: return  $Train, Valid, Test$             $\triangleright$  Return Final Splits

```

that NCNC [48] and EPS [44] integrate CNs into their framework and achieve SOTA performance. Furthermore, even on complex real-world datasets, CNs achieves competitive performance against more advanced neural models [21]. To control for the effect of CNs on shifted performance, the relevant splits will consider thresholds which include more CNs.

**(2) Shortest Path (SP):** SP captures a graph’s *global structural information*, thanks to the shortest-path between a given target and source node representing the most efficient path for reaching the target [39]. The shift in global structure caused by splitting data with SP can induce a scenario where a model must learn how two dissimilar nodes form a link with one another [11], which is comparable to the real-world scenario where two opponents choose to co-operate with one another [16, 41].

**(3) Preferential Attachment (PA):** PA captures the *scale-free property* of larger graphs by multiplying the degrees between two given nodes [5]. When applied to graph generation, PA produces synthetic Barabasi-Albert (BA) graphs which retain the scale-free property to effectively simulate the formation of new links in real-world graphs, such as the World Wide Web [3, 5]. Similar to CNs, the relevant PA splits will consider thresholds that integrate higher PA values.

### 3.2 Dataset Splitting Strategy

In the last subsection we described the different types of metrics to induce distribution shifts for LP. The metrics cover fundamental structural properties that influence the formation of new links. We now describe how we use these measures to split the dataset into train/validation/test splits to induce such shifts.

In order to build datasets with structural shift, we apply a given neighborhood heuristic to score each link. This score is then compared to a threshold ( $i_{train}, i_{valid}$ ) to categorize a link as a different

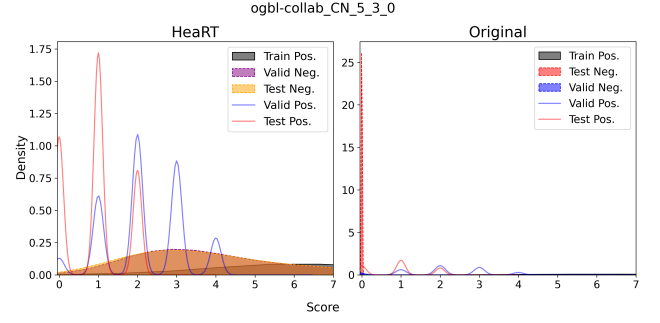


**Figure 1: The Common Neighbors distribution of the HeaRT versus the original testing and validation negative samples from LPShift’s ogbl-collab ‘CN - 5,3’ dataset.**

sample. As denoted in Alg. 1, the heuristic score of the link  $(u, v)$  is  $h(u, v)$ . The link falls into: training when  $h(u, v) < i_{train}$ , validation when  $i_{train} < h(u, v) \leq i_{valid}$ , and testing when  $h(u, v) > i_{valid}$ . The new training graph is constructed from the original OGB dataset [21]. Validation and testing samples are removed from the new training graph to prevent test-leakage and limited to 100-thousand edges maximum. The full algorithm is detailed in Algorithm 1 with additional details in Appendix C.

With Figure 2, we provide a small example of how splits are produced by our proposed splitting strategy. Specifically, Figure 2(a) demonstrates an outcome of the CN split labelled “CN - 1,2” where sampled edges pulled from the: black-dotted line = training (no CNs), red-dotted line = validation, (1 CN), and blue-dotted line = testing ( $\geq 2$  CNs). See Appendix C for information on Figure 2(b) and Figure 2(c).

To test how different LPShift thresholds impact performance, we adjust the  $i_{train}$  and  $i_{valid}$  thresholds to produce 3 varied CN and PA splits; as well as 2 varied SP splits. The variations in split thresholds were chosen based on two conditions. 1) Structural information within splits varies due to user-defined thresholds. In the “Forward” scenario (i.e. CN - 1,2), splits are given increasingly more structural information between training to validation, giving the model an easier time generalizing under testing. For the “Backward” scenario (i.e. CN - 2,1), stricter thresholds mean less structural information between validation to testing; making generalization difficult. 2) The final dataset split contains a sufficient number of samples. Each LPShift split requires enough split samples to allow model generalization. Given the limited number of SP split samples, the SP splits were limited to 2 variants. See Appendix C for more algorithmic details, and Appendix E for more information on LPShift’s efficiency and usefulness.

### 3.3 Why use HeaRT with LPShift?

It is common practice for most link prediction baselines to randomly-sample all negatives samples. However, random sampling is shown to be unrealistic, given that it is trivially-easy for a GNN4LP model trained via supervised learning to distinguish positive and negative samples based solely on the sample’s structure [31]. We demonstrate an example of this in the right subplot of Figure 1, where negative samples overwhelmingly contain 0 Common Neighbors

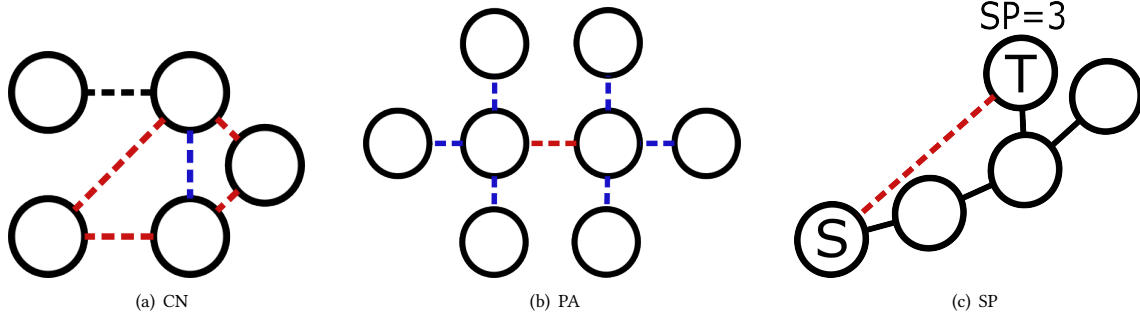


**Figure 2: An example of the three splitting strategies: (a) Common Neighbors, (b) Preferential-Attachment, (c) Shortest-Path. The dashed lines represent a cut on the source and target node that forms a given edge for our splitting strategy. The color of the line distinguishes the score assigned by the heuristic.**

versus HeaRT, whose negative samples are more closely-aligned with their respective positive samples. LPShift’s ability to induce distribution shift is explored further in Appendix Section G

#### 4 Why LPShift? A Theoretical Perspective

As neural models with backbone GNNs, GNN4LP relies on assumptions about the dataset’s underlying data distributions to learn representations for effective link prediction. Due to these assumptions, GNN4LP capture structural heuristics associated with link formation, such as LPFormer estimating Katz-Index [43]. LPShift undermines these assumptions through direct manipulation of the dataset sample distribution. We provide a theoretical perspective on this effect below:

*Notation:* We denote the node feature space as  $\mathbf{X} \in \mathbb{R}^{N \times F}$ , where  $F$  is the number of node features, and the adjacency matrix representing a given graph dataset as,  $\mathbf{A} \in \{0, 1\}^{N \times N}$ .

**Definition 4.1.** Let  $\mathcal{P}(\mathbf{H})$  represent a probability measure over  $\mathbf{H} = \text{GNN}(\mathbf{A}, \mathbf{X})$ . Given a sufficiently-large and i.i.d. dataset, it follows that an empirical measure on dataset subset estimated by GNN,  $\hat{\mathcal{P}}(\mathbf{H})$  over a subset of  $\mathbf{A}$  will capture the underlying distribution  $\mathcal{P}(\mathbf{H})$  for any dataset partition.

**THEOREM 4.2.** Let  $\Psi(u, v)$  represent a function to capture pairwise dependencies between a given edge,  $(u, v)$ , and subsequently partition a subset of edges from  $(\mathbf{A}, \mathbf{X})$  by their structure as determined by the output of  $\Psi(u, v)$ . Given this subset partitioned by  $\Psi(u, v)$ , it follows that the newly-partitioned samples violate the i.i.d. assumptions from Definition 4.1. Therefore, an empirical measure estimated by a GNN,  $\hat{\mathcal{P}}(\mathbf{H})$  over dataset subsets partitioned by  $\Psi(u, v)$  will not estimate one another, i.e.  $\hat{\mathcal{P}}^{\text{Train}}(\mathbf{H}) \neq \hat{\mathcal{P}}^{\text{Test}}(\mathbf{H})$ .

**PROOF.** Let  $\Psi(u, v)$  be a partition function over the dataset,  $(\mathbf{A}, \mathbf{X})$  which defines partitioned subset based on pairwise structures captured by  $\mathbf{A}$ . Given the i.i.d. assumption about dataset samples, it follows that for distinct partitions  $i \neq j$  and  $\mathbf{H} = \text{GNN}(\mathbf{A}, \mathbf{X})$ , it holds that  $\hat{\mathcal{P}}_{\Psi}^i(\mathbf{H}) \neq \hat{\mathcal{P}}_{\Psi}^j(\mathbf{H})$ . It then follows that  $\hat{\mathcal{P}}_{\Psi}^i(\mathbf{H}) \sim \mathcal{P}_{\Psi}^i(\mathbf{H})$  and  $\hat{\mathcal{P}}_{\Psi}^j(\mathbf{H}) \sim \mathcal{P}_{\Psi}^j(\mathbf{H})$ . Therefore,  $\hat{\mathcal{P}}_{\Psi}^i(\mathbf{H}) \neq \hat{\mathcal{P}}_{\Psi}^j(\mathbf{H}) \equiv \hat{\mathcal{P}}^{\text{Train}}(\mathbf{H}) \neq \hat{\mathcal{P}}^{\text{Test}}(\mathbf{H})$ .  $\square$

The supervised nature of training neural link prediction models with GNN backbones means that message-passing across training samples allows GNN4LP to observe and then model link formation to enhance downstream performance [7, 59]. However, Theorem 4.2 functions as a way of conditioning link formation dynamics within a given graph dataset so that necessary subsets are obscured. In effect, meaning the model gets a limited view on pairwise information contained within the dataset. As such, LPShift tests the hypothesis: *Can GNN4LP model structural heuristics for effective downstream performance in scenarios with limited structural information?* We verify this effect empirically in Section 5.

## 5 Experiments

To bridge the gap for GNN4LP generalizing under distribution shifts, this work addresses the following questions: **(RQ1)** Is the distribution shift induced by LPShift significant? **(RQ2)** Can SOTA GNN4LPs generalize under our proposed distribution shifts? **(RQ3)** Can current generalization methods further boost the performance of current methods? **(RQ4)** What components of the proposed distribution shift are affecting the LP model’s performance?

### 5.1 Experimental Setup

**Datasets:** We consider 16 “Forward” and “Backward” LPShift splits for the following 3 OGB datasets [21]: ppa, ddi, and collab, for a total of 48 tested splits. The resulting datasets represent tasks in three separate domains and three shifted scenarios, allowing a comprehensive study of LP generalization under distribution shift. For all datasets, we create multiple splits corresponding to each structural property detailed in Section 3.2. For the “Forward” split, denoted as  $(X, Y, Z)$ , an increase in  $Y$  and  $Z$  indicates more structural information available to the training adjacency matrix. The “Backward” split swaps the training and testing splits from their counterpart in the “Forward” split, resulting in the training adjacency matrix losing access to structural information as  $X$  and  $Y$  increase. See Appendix J for more details.

**GNN4LP Methods:** We test multiple SOTA GNN4LP methods including: NCNC [48], BUDDY [8], LPFormer [43], SEAL [61] and Neo-GNN [58]. We further consider GCN [25] as a simpler GNN

baseline, along with the Resource Allocation (RA) [65] heuristic. All models were selected based on their benchmark performance with the original OGB datasets [21] and their architectural differences detailed in Section 2.

**Graph-Specific Generalization Methods:** We also test the performance of BUDDY with multiple generalization techniques. This includes DropEdge [37], which randomly removes a portion of edges from the training adjacency matrix. Edge Proposal Sets (EPS) [44], which uses paired LP models to filter and rank top-k edges to insert as Common Neighbors in the training adjacency matrix. Lastly, we consider Topological Concentration (TC) [49], which re-weights the edges within the training adjacency matrix based on the structural information.

**Traditional Generalization Methods:** The final round of tests applies: IRM [4], VREx [28], GroupDRO [40], DANN [14], and DeepCORAL [47] as generalization methods to GCN. Given that LPShift splits graph data directly on the sample structure, all tests with traditional generalization methods treat training samples as an environment,  $\mathcal{E} = \{e_1, \dots, e_N\}$  composed of  $N$  environmental subsets, where each subset is binned based on their neighborhood heuristic; as demonstrated for CNs in Figure 3. This binning of environmental subsets forces traditional generalization methods to target graph structure, controlling for the method’s ability to improve performance under structural shift induced by LPShift.

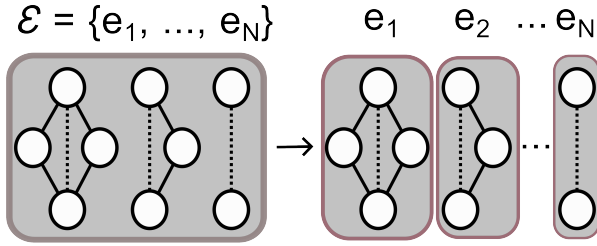


Figure 3: The original environment of dataset samples split into subsets by their CN heuristic scores.

**Evaluation Setting:** We consider the standard evaluation procedure in LP, in which every positive validation/test sample is compared against  $M$  negative samples. The goal is that the model should output a higher score (i.e., probability) for positive sample than the negatives. To create the negatives, we make use of the HearT evaluation setting [31] which generates  $M$  negatives samples *per positive sample* according to a set of common LP heuristics. In our study, we set  $M = 250$  and use CNs coupled with PPR as the heuristic in HearT.

**Evaluation Metrics:** We evaluate all methods using the mean reciprocal rank (MRR) across multiple Hits@K ranking metrics,  $K = \{1, 3, 5, 10, 20, 50, 100\}$ .

**Hyperparameters:** All methods were tuned on permutations of learning rates in  $\{1e^{-2}, 1e^{-3}\}$  and dropout in  $\{0.1, 0.3\}$ . Each model was trained and tested over five seeds to obtain the mean and standard deviations of their results. Given the significant time complexity of training and testing on the customized ogbl-ppa

datasets, NCNC and LPFormer were tuned on a single seed, followed by an evaluation of the tuned model on five separate seeds. Additional hyperparameter tuning details are included in Appendix Section J.

## 5.2 Results for GNN4LP

In order to provide a unified perspective on how distribution shift affects link prediction models, each GNN4LP method was trained and tested across five seeded runs on versions of ogbl-collab, ppa, and ddi split by: Common Neighbors, Shortest-Path, and Preferential-Attachment. Examining the results, we have the following three key observations.

**Observation 1: Drastic Changes in Model Performance.** As shown in Table 1, the majority of synthetic splits generated by LPShift reduce model performance significantly below the original HearT standard [31]. This is especially pronounced in denser graphs like ogbl-ppa and ogbl-ddi, indicating that LPShift affects the varied structures of graph data which then reduces downstream performance. The only exception is ogbl-collab, where: RA, NCNC, LPFormer, and SEAL experience measurable improvements over the HearT baseline. Given ogbl-collab’s lack of density, relative to ogbl-ppa and ogbl-ddi, there are considerations about how LPShift induces a covariate shift to features [26], especially where structure is correlated to the feature distribution.

Additional analysis shown in Figure 6 and 7 indicates how dataset structure relates to the performance effects of LPShift. Furthermore, to quantify the extent of how the node features correlate with LPShift, we measure the cosine similarity of each split’s feature distribution. These results are shown in Appendix D.

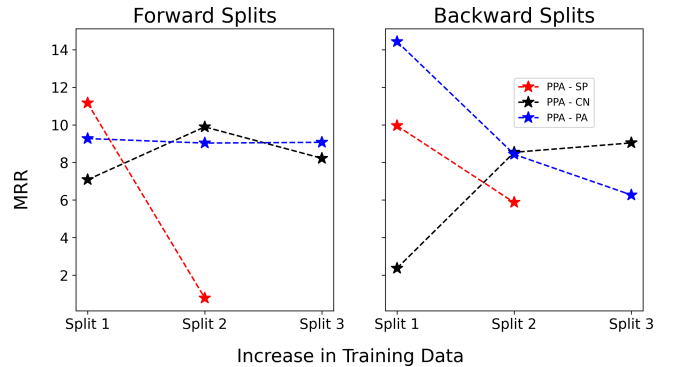


Figure 4: The mean scores of the best-performing GNN4LP models on LPShift’s ogbl-ppa dataset. Each line represents a given dataset and split, arranged uniformly between figures. In the case of decreasing performance, the model with the highest average values was selected.

**Observation 2: Performance Differs By Split Type and Threshold.** As shown in Figure 4, regardless of whether a model is tested on a “Forward” or “Backward” split of ogbl-ppa; the change in structural information for each subsequent split gradually changes a model’s performance. On the “CN” split, a stark increase is seen between “Split 1” and “Split 2”, indicating that more structural information from training and validation improves GNN4LP performance [48], even on dense datasets like ogbl-ppa. The fact that these



**Table 1: The average percent change in MRR for each tuned model versus the HeaRT benchmark [31], sorted by dataset then LPShift split and direction.**

Dataset	Split	Direction	GCN	RA	NCNC	NeoGNN	BUDDY	LPFormer	SEAL
PPA	CN	Forward	-69.4%	-84.0%	-84.5%	-77.0%	-84.8%	-91.2%	-67.5%
		Backward	-91.4%	-96.9%	-75.0%	-96.3%	-92.0%	-88.3%	-96.3%
	SP	Forward	-78.9%	-7.5%	-82.2%	-72.4%	-83.3%	-81.7%	-75.1%
		Backward	-75.4%	-97.9%	-89.8%	-86.5%	-76.6%	-91.4%	-96.6%
	PA	Forward	-84.3%	-88.5%	-85.4%	-35.0%	-84.6%	-77.3%	-87.4%
		Backward	-89.6%	-78.5%	-74.0%	-77.8%	-90.3%	-75.9%	-86.8%
DDI	CN	Forward	-66.1%	-50.5%	>24hr	-85.3%	-82.4%	-93.1%	-89.9%
		Backward	-91.2%	-93.9%	>24hr	-80.7%	-91.2%	-73.4%	-93.0%
	PA	Forward	-84.0%	-56.2%	>24hr	-86.0%	-85.3%	-97.1%	-87.8%
		Backward	-80.5%	-60.8%	>24hr	-75.1%	-83.9%	-74.4%	-74.4%
Collab	CN	Forward	-5.7%	+8.8%	-41.5%	-49.8%	-49.1%	+89.6%	-29.8%
		Backward	-69.6%	-74.8%	-64.1%	-79.6%	-87.0%	-37.7%	-81.6%
	SP	Forward	-23.0%	+20.4%	-49.0%	-72.7%	-49.7%	+33.2%	-90.7%
		Backward	-7.7%	-97.7%	-95.6%	-83.8%	-84.0%	-67.1%	-96.2%
	PA	Forward	-17.5%	+3.9%	-27.1%	-35.7%	-50.3%	+117.5%	-2.4%
		Backward	-6.5%	+41.6%	+1.9%	-77.1%	-44.7%	+203.4%	+52.9%

results include splits produced by Preferential-Attachment, Global Structural Information (SP), and Local Structural Information (CN) indicates the effect of *any* change in structural information when training LP models [35].

**Observation 3: Performance Impact Varies by Model.** All raw MRR scores are stored in Appendix Section H within Tables 7 to 9. We can make the following observations by split type. **Common Neighbors:** Most models fail to generalize on the “Backward” CN splits. However, once more Common Neighbors are made available in the CN - 4,2 and CN - 5,3 splits; NCNC performs 2 to 3 times better than other GNN4LP models. Therefore, indicating that it is possible to generalize with limited local information. **Shortest-Path:** GNN4LP Models which rely more on local structural information (i.e. NCNC, LPFormer, and SEAL) typically suffer more under the “Backward” SP splits, resulting in the models performing 2x to 4x worse than BUDDY or GCN. Therefore, indicating the necessity for models to adapt in scenarios with an absence of local structural information. **Preferential-Attachment:** LPFormer performance on the PA split is 2 times higher than HeaRT’s ogbl-collab [31], but reduces drastically on LPShift’s ogbl-ppa or ogbl-ddi. Therefore, indicating the impact that structural shift incurs with the increasing density of datasets.

### 5.3 Results for Generalization Methods

In this section, we apply DropEdge [37], EPS [44], and TC [64] on the previously benchmarked BUDDY [8] to determine the feasibility of improving the LP models’ generalization under LPShift.

**Observation 1: Graph-Specific Generalization Methods Can Help.** As demonstrated in Table 2, the two generalization methods specific to LP: TC [49] and EPS [44] fail to increase performance under LPShift in the “Forward” CN and PA splits. However, the

methods do improve performance, as indicated by the “Backward” DDI split, where both EdgeDrop and EPS increase model performance by 3.87% and 7.5%, respectively. This is likely due to the exceptionally dense nature of DDI, where numerous high-degree nodes are likely made more relevant to performance through: 1) the removal of edges from EdgeDrop or 2) connecting relevant neighbors with EPS. To validate this, we calculate Earth Mover’s Distance (EMD) [38] between the heuristic scores of the training and testing splits before and after applying the generalization methods. EPS injects CNs into the training adjacency matrix, significantly altering the training and testing distributions. This drastic change is indicated in Figures 8 and 5 with the near-perfect EMD scores of EPS. Such a change in EMD and the Table 2 results, demonstrates that generalizing under LPShift can be achieved with targeted augmentations to the graph data structure. However, EdgeDrop has relatively-minimal effect on the EMD scores, indicating that non-targeted augmentations can function on highly-dense datasets.

TC often decreases performance on “Forward” splits. This is likely due to LPShift’s distinct split thresholds; meaning there is limited structural overlap between sample distributions. As such, TC can’t re-weight the training adjacency matrix for improved generalization to neighborhood information [29, 49]. This result runs contrary to current work, where re-weighting is effective for handling distribution shifts in other graph tasks [66] and computer vision [13]. However, the “Backward” CN and SP splits indicate consistent performance increases induced by TC.

**Observation 2: Traditional Generalization Methods Work in Limited Scenarios.** As shown in Table 3, any of the generalization methods tested on the “Forward” split rarely improve performance. IRM and DRO often reduce performance the most, sometimes by more than 10% MRR. All methods encounter more

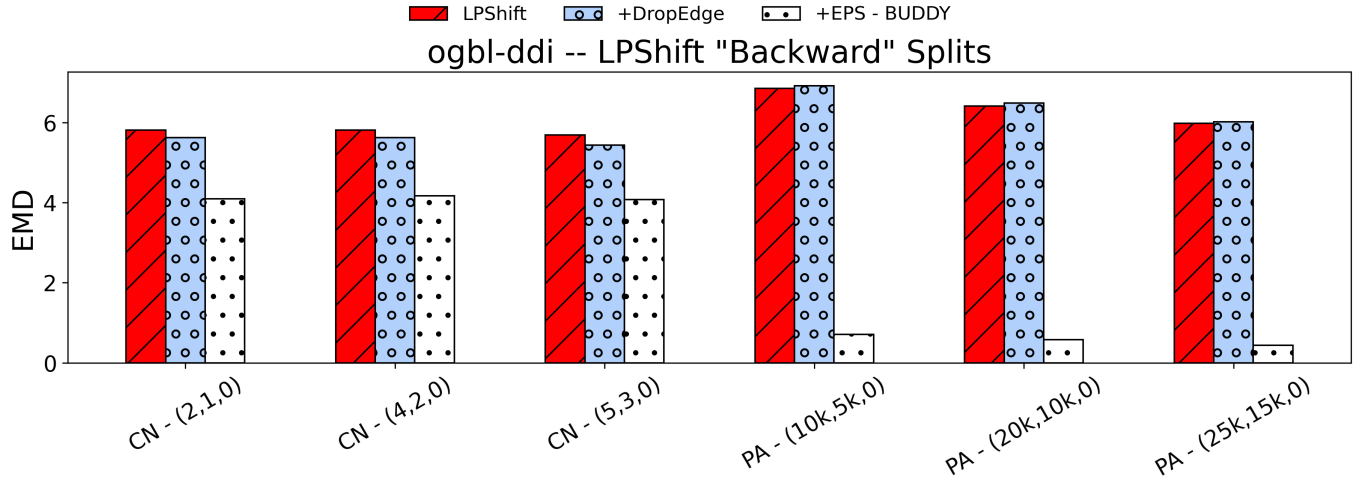


Figure 5: The EMD values calculated between the heuristic scores of training and testing samples. *Note:* The tested heuristics correspond to their labelled splits, so as to simulate the dataset splitting.

Table 2: The raw MRR change for the BUDDY results in Table 1, after applying graph-specific generalization methods, averaged over LPShift splits.

	Forward			Backward		
	CN	SP	PA	CN	SP	PA
Collab						
ED	-0.5	-1.6	-0.11	-0.72	-1.09	+0.36
TC	-3.63	-8.02	-2.26	+1.29	+1.34	-7.38
EPS	-4.28	-7.82	-4.46	+1.38	+1.45	-8.55
PPA						
ED	-0.02	+1.31	+0.003	+0.003	0.0	+0.006
TC	-1.31	+0.86	-0.90	+1.27	+1.58	-1.09
EPS	-1.12	+1.14	-1.02	+1.06	+2.2	-0.91
DDI						
ED	0.0	-	0.0	0.0	-	+3.87
TC	-1.17	-	0.0	-0.12	-	-0.46
EPS	-0.86	-	-0.58	+1.19	-	+7.5

consistent performance improvements on the "Backward" ogbl-ppa and ogbl-ddi splits. Given that all generalization methods are trained on environmental subsets defined by structural heuristics, it follows that the traditional generalization methods improve performance under LPShift when given sample subsets with distinct and diverse structural patterns. Future work could explore this idea further by applying different heuristic scores to each environmental subset.

## 5.4 Discussion

**Does GNN4LP generalize and do generalization methods work?** As detailed in Table 1, LPShift significantly reduces the performance for a majority of LP methods versus HeaRT. This is

Table 3: The raw MRR change for the GCN results in Table 1, after applying traditional generalization methods, averaged over LPShift splits.

	Forward			Backward		
	CN	SP	PA	CN	SP	PA
Collab						
IRM	-10.62	-8.51	-6.74	-2.66	-2.18	-14.86
VREx	-0.53	+0.39	+2.12	+0.31	+0.02	-1.29
DRO	-11.96	-7.76	-7.41	-2.51	-1.32	-13.66
DANN	-0.13	+0.74	+2.35	+0.39	+3.36	-1.75
CORAL	-0.54	+0.36	+2.02	+0.25	+3.32	-1.29
PPA						
IRM	-6.16	+0.02	-0.15	+0.3	-4.51	+0.53
VREx	-0.9	+0.08	+0.07	+0.79	-0.17	+0.03
DRO	-5.86	-1.87	-0.73	+0.45	-4.48	+0.83
DANN	-0.84	+0.13	+0.65	+0.72	-0.12	-0.45
CORAL	-0.91	+0.02	+0.37	+0.71	-0.17	-0.51
DDI						
IRM	-3.44	-	-0.56	+3.24	-	+3.26
VREx	-3.68	-	-0.66	+2.76	-	+1.56
DRO	-3.47	-	-0.77	+3.16	-	+1.89
DANN	-3.55	-	-0.66	+3.26	-	+1.59
CORAL	-3.72	-	-0.62	+2.74	-	+1.18

especially notable given the difficulty HeaRT imposes on the original benchmark setting [21]. This observation coupled with the limited success of all generalization methods on "Forward" splits in Tables 2 and 3 shows the difficulty posed on LP models when trained with limited structural information relative to evaluation samples.

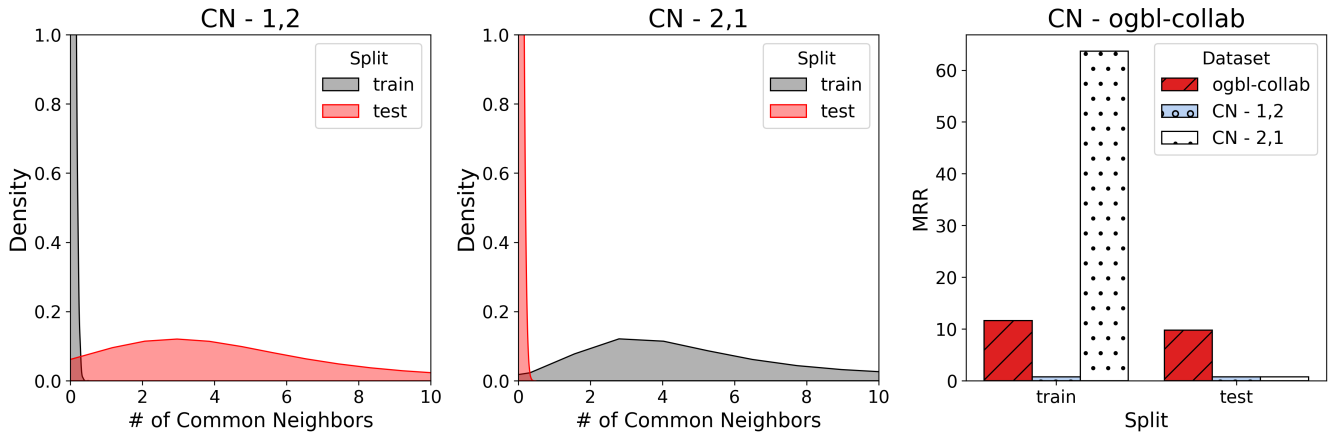


**Figure 6:** Three subplots corresponding to: 1.) the 'CN - 1,2' LPShift on ogbl-collab 2.) the 'CN - 2,1' LPShift on ogbl-collab 3.) CN predictor performance for the original ogbl-collab, 'CN - 1,2', and 'CN - 2,1' splits.

**How is the proposed distribution shift affecting performance?** In order to verify that LPShift's effect on dataset structure is significant and can be correlated to performance, we follow a similar analysis conducted in [48], as shown in Figure 6. In which, CN's predictive performance is measured and compared under the "Forward" and "Backward" LPShift. We choose CN as the predictor given that it relies on directly ranking the given dataset samples by structure in order to predict if a link forms; meaning performance is sensitive to a change in dataset structure.

The first two subplots in Figure 6 depict the density estimates of the CN distribution for the CN - 1,2 and CN - 2,1 LPShift splits of the ogbl-collab dataset. The third subplot depicts the performance of CN on the datasets depicted in the first two subplots.

Given the targeted effect of LPShift on dataset structure, the reduced performance (1% MRR) of the CN ranking, as shown in Figure 6, on the CN - 1,2 split is due to the lack of structural information in the training split (CN = 0), limiting its ability to rank valid and test samples with  $>1$  CNs. The structure-to-performance link is clearer in the CN - 2,1 scenario: where training with 2+ CNs yields 60% MRR, but fails to generalize on test samples with zero CNs, shown by the 1% MRR score. Given that all GNN4LP models incorporate neighborhood/structural information into their architectures [48], it follows that GNN4LP's reduced performance under LPShift is due to the splitting strategy enforcing a scenario where models must generalize to dataset samples drawn from a different distributions.

## 6 Conclusion

This work proposes LPShift, a simple dataset splitting strategy for inducing structural shift relevant for link prediction. The effect of this structural shift was then benchmarked on 16 shifted versions of ogbl-collab, ppa, and ddi, posing a unique challenge for SOTA GNN4LP models and generalization methods versus the HeaRT. Further analysis indicates that current generalization methods improve performance under LPShift in scenarios with diverse pairwise structures amongst training samples. As such, LPShift demonstrates that GNN4LP is vulnerable to distribution shift induced by pairwise

heuristic. Given the severity of structural shift induced by LPShift, future work can consider relaxing the threshold between sample distributions or consider mixing structural heuristics to better mimic real-world distribution shift and the complexities therein.

## References

- [1] Khushnood Abbas, Alireza Abbasi, Shi Dong, Ling Niu, Laihang Yu, Bolun Chen, Shi-Min Cai, and Qambar Hasan. 2021. Application of network link prediction in drug discovery. *BMC bioinformatics* 22 (2021), 1–21.
- [2] Lada A Adamic and Eytan Adar. 2003. Friends and neighbors on the web. *Social networks* 25, 3 (2003), 211–230.
- [3] Réka Albert and Albert-László Barabási. 2002. Statistical mechanics of complex networks. *Reviews of Modern Physics* 74, 1 (Jan. 2002), 47–97. doi:10.1103/revmodphys.74.47
- [4] Martin Arjovsky, Léon Bottou, Ishaan Gulrajani, and David Lopez-Paz. 2019. Invariant risk minimization. *arXiv preprint arXiv:1907.02893* (2019).
- [5] Albert-László Barabási and Réka Albert. 1999. Emergence of Scaling in Random Networks. *Science* 286, 5439 (1999), 509–512. doi:10.1126/science.286.5439.509 arXiv:https://www.science.org/doi/pdf/10.1126/science.286.5439.509
- [6] Beatrice Bevilacqua, Yangze Zhou, and Bruno Ribeiro. 2021. Size-invariant graph representations for graph classification extrapolations. In *International Conference on Machine Learning*. PMLR, 837–851.
- [7] Michael M Bronstein, Joan Bruna, Taco Cohen, and Petar Veličković. 2021. Geometric deep learning: Grids, groups, graphs, geodesics, and gauges. *arXiv preprint arXiv:2104.13478* (2021).
- [8] Benjamin Paul Chamberlain, Sergey Shirobokov, Emanuele Rossi, Fabrizio Frasca, Thomas Markovich, Nils Hammerla, Michael M Bronstein, and Max Hansmire. 2022. Graph Neural Networks for Link Prediction with Subgraph Sketching. *arXiv preprint arXiv:2209.15486* (2022).
- [9] Mucong Ding, Kezhi Kong, Jiuhai Chen, John Kirchenbauer, Micah Goldblum, David Wipf, Furong Huang, and Tom Goldstein. 2021. A Closer Look at Distribution Shifts and Out-of-Distribution Generalization on Graphs. In *NeurIPS 2021 Workshop on Distribution Shifts: Connecting Methods and Applications*. https://openreview.net/forum?id=XvgPGWazqRH
- [10] Kaiwen Dong, Yijun Tian, Zhichun Guo, Yang Yang, and Nitesh Chawla. 2022. Fakeedge: Alleviate dataset shift in link prediction. In *Learning on Graphs Conference*. PMLR, 56–1.
- [11] Anna Evtushenko and Jon Kleinberg. 2021. The paradox of second-order homophily in networks. *Scientific Reports* 11, 1 (2021), 13360.
- [12] Wenqi Fan, Yao Ma, Qing Li, Yuan He, Eric Zhao, Jiliang Tang, and Dawei Yin. 2019. Graph neural networks for social recommendation. In *The world wide web conference*. 417–426.
- [13] Tongtong Fang, Nan Lu, Gang Niu, and Masashi Sugiyama. 2020. Rethinking importance weighting for deep learning under distribution shift. *Advances in neural information processing systems* 33 (2020), 11996–12007.
- [14] Yaroslav Ganin, Evgeniya Ustinova, Hana Ajakan, Pascal Germain, Hugo Larochelle, François Laviolette, Mario March, and Victor Lempitsky. 2016. Domain-adversarial training of neural networks. *Journal of machine learning*



- research 17, 59 (2016), 1–35.
- [15] Yuan Gao, Xiang Wang, Xiangnan He, Zhengguang Liu, Huamin Feng, and Yongdong Zhang. 2023. Alleviating structural distribution shift in graph anomaly detection. In *Proceedings of the Sixteenth ACM International Conference on Web Search and Data Mining*. 357–365.
  - [16] Mark Granovetter. 1978. Threshold models of collective behavior. *American journal of sociology* 83, 6 (1978), 1420–1443.
  - [17] Shurui Gui, Xiner Li, Limei Wang, and Shuiwang Ji. 2022. Good: A graph out-of-distribution benchmark. *Advances in Neural Information Processing Systems* 35 (2022), 2059–2073.
  - [18] Yuxin Guo, Cheng Yang, Yuluo Chen, Jixi Liu, Chuan Shi, and Junping Du. 2023. A Data-centric Framework to Endow Graph Neural Networks with Out-Of-Distribution Detection Ability. In *Proceedings of the 29th ACM SIGKDD Conference on Knowledge Discovery and Data Mining*. 638–648.
  - [19] J.L. Hodges Jr. 1958. The significance probability of the Smirnov two-sample test. *Arkiv för matematik* 3, 5 (1958), 469–486.
  - [20] Petter Holme and Beom Jun Kim. 2002. Growing scale-free networks with tunable clustering. *Physical review E* 65, 2 (2002), 026107.
  - [21] Weihua Hu, Matthias Fey, Marinka Zitnik, Yuxiao Dong, Hongyu Ren, Bowen Liu, Michele Catasta, and Jure Leskovec. 2020. Open graph benchmark: Datasets for machine learning on graphs. *Advances in neural information processing systems* 33 (2020), 22118–22133.
  - [22] Yuanfeng Ji, Lu Zhang, Jiaxiang Wu, Bingzhe Wu, Long-Kai Huang, Tingyang Xu, Yu Rong, Lanqing Li, Jie Ren, Ding Xue, et al. 2022. DrugOOD: Out-of-Distribution (OOD) Dataset Curator and Benchmark for AI-aided Drug Discovery—A Focus on Affinity Prediction Problems with Noise Annotations. *arXiv preprint arXiv:2201.09637* (2022).
  - [23] Wei Jin, Tong Zhao, Jiayuan Ding, Yozen Liu, Jiliang Tang, and Neil Shah. 2022. Empowering graph representation learning with test-time graph transformation. *arXiv preprint arXiv:2210.03561* (2022).
  - [24] Thomas N Kipf and Max Welling. 2016. Variational graph auto-encoders. *arXiv preprint arXiv:1611.07308* (2016).
  - [25] Thomas N. Kipf and Max Welling. 2017. Semi-Supervised Classification with Graph Convolutional Networks. In *International Conference on Learning Representations (ICLR)*.
  - [26] Pang Wei Koh, Shiori Sagawa, Henrik Marklund, Sang Michael Xie, Marvin Zhang, Akshay Balsubramani, Weihua Hu, Michihiro Yasunaga, Richard Lanus, Phillips, Irena Gao, et al. 2021. Wilds: A benchmark of in-the-wild distribution shifts. In *International conference on machine learning*. PMLR, 5637–5664.
  - [27] István A Kovács, Katja Luck, Kerstin Spirohn, Yang Wang, Carl Pollis, Sadie Schlabach, Wenting Bian, Dae-Kyung Kim, Nishka Kishore, Tong Hao, et al. 2019. Network-based prediction of protein interactions. *Nature communications* 10, 1 (2019), 1240.
  - [28] David Krueger, Ethan Caballero, Joern-Henrik Jacobsen, Amy Zhang, Jonathan Binas, Dinghui Zhang, Remi Le Priol, and Aaron Courville. 2021. Out-of-distribution generalization via risk extrapolation (rex). In *International conference on machine learning*. PMLR, 5815–5826.
  - [29] Haoyang Li, Xin Wang, Ziwei Zhang, and Wenwu Zhu. 2022. Ood-gnn: Out-of-distribution generalized graph neural network. *IEEE Transactions on Knowledge and Data Engineering* (2022).
  - [30] Haoyang Li, Xin Wang, Ziwei Zhang, and Wenwu Zhu. 2022. Out-of-distribution generalization on graphs: A survey. *arXiv preprint arXiv:2202.07987* (2022).
  - [31] Juanhui Li, Harry Shomer, Haitao Mao, Shenglai Zeng, Yao Ma, Neil Shah, Jiliang Tang, and Dawei Yin. 2024. Evaluating graph neural networks for link prediction: Current pitfalls and new benchmarking. *Advances in Neural Information Processing Systems* 36 (2024).
  - [32] David Liben-Nowell and Jon Kleinberg. 2003. The link prediction problem for social networks. In *Proceedings of the twelfth international conference on Information and knowledge management*. 556–559.
  - [33] Yankai Lin, Zhiyuan Liu, Maosong Sun, Yang Liu, and Xuan Zhu. 2015. Learning entity and relation embeddings for knowledge graph completion. In *Proceedings of the AAAI conference on artificial intelligence*, Vol. 29.
  - [34] Haitao Mao, Zhikai Chen, Wei Jin, Haoyu Han, Yao Ma, Tong Zhao, Neil Shah, and Jiliang Tang. 2024. Demystifying Structural Disparity in Graph Neural Networks: Can One Size Fit All? *Advances in Neural Information Processing Systems* 36 (2024).
  - [35] Haitao Mao, Juanhui Li, Harry Shomer, Bingheng Li, Wenqi Fan, Yao Ma, Tong Zhao, Neil Shah, and Jiliang Tang. 2024. Revisiting Link Prediction: a data perspective. In *The Twelfth International Conference on Learning Representations*.
  - [36] Mark EJ Newman. 2001. Clustering and preferential attachment in growing networks. *Physical review E* 64, 2 (2001), 025102.
  - [37] Yu Rong, Wenbing Huang, Tingyang Xu, and Junzhou Huang. 2020. DropEdge: Towards Deep Graph Convolutional Networks on Node Classification. In *International Conference on Learning Representations*. <https://openreview.net/forum?id=Hkx1qkrKPr>
  - [38] Y. Rubner, C. Tomasi, and L.J. Guibas. 1998. A metric for distributions with applications to image databases. In *Sixth International Conference on Computer Vision (IEEE Cat. No.98CH36271)*. 59–66. doi:10.1109/ICCV.1998.710701
  - [39] Stuart Russell and Peter Norvig. 2009. *Artificial Intelligence: A Modern Approach* (3rd ed.). Prentice Hall Press, USA.
  - [40] Shiori Sagawa, Pang Wei Koh, Tatsunori B Hashimoto, and Percy Liang. 2019. Distributionally robust neural networks for group shifts: On the importance of regularization for worst-case generalization. *arXiv preprint arXiv:1911.08731* (2019).
  - [41] Thomas C Schelling. 1978. *Micromotives and Macrobehavior* WW Norton & Company. New York, NY (1978).
  - [42] Zhihao Shi, Jie Wang, Fanghua Lu, Hanzhu Chen, Defu Lian, Zheng Wang, Jieping Ye, and Feng Wu. 2023. Label Deconvolution for Node Representation Learning on Large-scale Attributed Graphs against Learning Bias. *arXiv preprint arXiv:2309.14907* (2023).
  - [43] Harry Shomer, Yao Ma, Haitao Mao, Juanhui Li, Bo Wu, and Jiliang Tang. 2024. LPFormer: an adaptive graph transformer for link prediction. In *Proceedings of the 30th ACM SIGKDD Conference on Knowledge Discovery and Data Mining*. 2686–2698.
  - [44] Abhay Singh, Qian Huang, Sijia Linda Huang, Omkar Bhalerao, Horace He, Ser-Nam Lim, and Austin R Benson. 2021. Edge proposal sets for link prediction. *arXiv preprint arXiv:2106.15810* (2021).
  - [45] Balasubramaniam Srinivasan and Bruno Ribeiro. 2019. On the Equivalence between Positional Node Embeddings and Structural Graph Representations. In *International Conference on Learning Representations*.
  - [46] Yongduo Sui, Qitian Wu, Jiancan Wu, Qing Cui, Longfei Li, Jun Zhou, Xiang Wang, and Xiangnan He. 2024. Unleashing the power of graph data augmentation on covariate distribution shift. *Advances in Neural Information Processing Systems* 36 (2024).
  - [47] Baochen Sun and Kate Saenko. 2016. Deep coral: Correlation alignment for deep domain adaptation. In *Computer Vision—ECCV 2016 Workshops: Amsterdam, The Netherlands, October 8–10 and 15–16, 2016, Proceedings, Part III 14*. Springer, 443–450.
  - [48] Xiyuan Wang, Haotong Yang, and Muhao Zhang. 2023. Neural Common Neighbor with Completion for Link Prediction. In *The Twelfth International Conference on Learning Representations*.
  - [49] Yu Wang, Tong Zhao, Yuying Zhao, Yunchao Liu, Xueqi Cheng, Neil Shah, and Tyler Derr. 2023. A Topological Perspective on Demystifying GNN-Based Link Prediction Performance. *arXiv preprint arXiv:2310.04612* (2023).
  - [50] Lanning Wei, Huan Zhao, Quanming Yao, and Zhiqiang He. 2021. Pooling Architecture Search for Graph Classification. In *Proceedings of the 30th ACM International Conference on Information and Knowledge Management (CIKM '21)*. ACM. doi:10.1145/3459637.3482285
  - [51] Olivia Wiles, Sven Gowal, Florian Stimpberg, Sylvestre-Alvise Rebuffi, Ira Ktena, Krishnamurthy Dvijotham, and A. Cemgil. 2021. A Fine-Grained Analysis on Distribution Shift. *ArXiv abs/2110.11328* (2021).
  - [52] Qitian Wu, Yiting Chen, Chenxiao Yang, and Junchi Yan. 2023. Energy-based out-of-distribution detection for graph neural networks. *arXiv preprint arXiv:2302.02914* (2023).
  - [53] Qitian Wu, Fan Nie, Chenxiao Yang, Tianyi Bao, and Junchi Yan. 2024. Graph Out-of-Distribution Generalization via Causal Intervention. In *Proceedings of the ACM on Web Conference 2024*. 850–860.
  - [54] Qitian Wu, Hengrui Zhang, Junchi Yan, and David Wipf. 2022. Handling Distribution Shifts on Graphs: An Invariance Perspective. In *International Conference on Learning Representations (ICLR)*.
  - [55] Huaxiu Yao, Caroline Choi, Bochuan Cao, Yoonho Lee, Pang Wei W Koh, and Chelsea Finn. 2022. Wild-Time: A Benchmark of in-the-Wild Distribution Shift over Time. In *Advances in Neural Information Processing Systems*. S. Koyejo, S. Mohamed, A. Agarwal, D. Belgrave, K. Cho, and A. Oh (Eds.), Vol. 35. Curran Associates, Inc., 10309–10324. [https://proceedings.neurips.cc/paper\\_files/paper/2022/file/43119db5d59f07cc08fca7ba6820179a-Paper-Datasets\\_and\\_Benchmarks.pdf](https://proceedings.neurips.cc/paper_files/paper/2022/file/43119db5d59f07cc08fca7ba6820179a-Paper-Datasets_and_Benchmarks.pdf)
  - [56] Huaxiu Yao, Yu Wang, Sai Li, Linjun Zhang, Weixin Liang, James Zou, and Chelsea Finn. 2022. Improving Out-of-Distribution Robustness via Selective Augmentation. In *Proceedings of the 39th International Conference on Machine Learning (Proceedings of Machine Learning Research, Vol. 162)*, Kamalika Chaudhuri, Stefanie Jegelka, Le Song, Csaba Szepesvari, Gang Niu, and Sivan Sabato (Eds.). PMLR, 25407–25437. <https://proceedings.mlr.press/v162/yao22b.html>
  - [57] Zhuoning Yuan, Yan Yan, Milan Sonka, and Tianbao Yang. 2021. Large-scale Robust Deep AUC Maximization: A New Surrogate Loss and Empirical Studies on Medical Image Classification. *arXiv:2012.03173 [cs.LG]*
  - [58] Seongjun Yun, Seoyoon Kim, Junhyun Lee, Jaewoo Kang, and Hyunwoo J Kim. 2021. Neo-gnns: Neighborhood overlap-aware graph neural networks for link prediction. *Advances in Neural Information Processing Systems* 34 (2021), 13683–13694.
  - [59] Matej Žečević, Devendra Singh Dhami, Petar Veličković, and Kristian Kersting. 2021. Relating graph neural networks to structural causal models. *arXiv preprint arXiv:2109.04173* (2021).
  - [60] Muhao Zhang and Yixin Chen. 2018. Link prediction based on graph neural networks. *Advances in neural information processing systems* 31 (2018).
  - [61] Muhao Zhang, Pan Li, Yinglong Xia, Kai Wang, and Long Jin. 2021. Labeling trick: A theory of using graph neural networks for multi-node representation learning.

- Advances in Neural Information Processing Systems* 34 (2021), 9061–9073.
- [62] Zeyang Zhang, Xin Wang, Ziwei Zhang, Haoyang Li, Zhou Qin, and Wenwu Zhu. 2022. Dynamic graph neural networks under spatio-temporal distribution shift. *Advances in neural information processing systems* 35 (2022), 6074–6089.
  - [63] Jianan Zhao, Meng Qu, Chaozhuo Li, Hao Yan, Qian Liu, Rui Li, Xing Xie, and Jian Tang. 2022. Learning on large-scale text-attributed graphs via variational inference. *arXiv preprint arXiv:2210.14709* (2022).
  - [64] Jianan Zhao, Meng Qu, Chaozhuo Li, Hao Yan, Qian Liu, Rui Li, Xing Xie, and Jian Tang. 2023. Learning on Large-scale Text-attributed Graphs via Variational Inference. *arXiv:2210.14709* [cs.LG]
  - [65] Tao Zhou, Linyuan Lü, and Yi-Cheng Zhang. 2009. Predicting missing links via local information. *The European Physical Journal B* 71 (2009), 623–630.
  - [66] Xiao Zhou, Yong Lin, Renjie Pi, Weizhong Zhang, Renzhe Xu, Peng Cui, and Tong Zhang. 2022. Model agnostic sample reweighting for out-of-distribution learning. In *International Conference on Machine Learning*. PMLR, 27203–27221.
  - [67] Yangze Zhou, Gitta Kutyniok, and Bruno Ribeiro. 2022. OOD link prediction generalization capabilities of message-passing GNNs in larger test graphs. *Advances in Neural Information Processing Systems* 35 (2022), 20257–20272.
  - [68] Jing Zhu, Yuhang Zhou, Vassilis N Ioannidis, Shengyi Qian, Wei Ai, Xiang Song, and Danai Koutra. 2024. Pitfalls in Link Prediction with Graph Neural Networks: Understanding the Impact of Target-link Inclusion & Better Practices. In *Proceedings of the 17th ACM International Conference on Web Search and Data Mining*. 994–1002.
  - [69] Zhaocheng Zhu, Zuobai Zhang, Louis-Pascal Xhonneux, and Jian Tang. 2021. Neural bellman-ford networks: A general graph neural network framework for link prediction. *Advances in Neural Information Processing Systems* 34 (2021), 29476–29490.

## A Realistic Scenarios for Structural Shift in Link Prediction

- **Adversarial Recommender Systems = Shortest-Path:** A company may want to understand which products to *avoid* showing to a potential customer without need to hear the user’s preferences directly. In this scenario, global information, as captured by Shortest-Path, becomes the most valuable for the specific use-case.
- **Social Recommender Systems = Preferential-Attachment:** A video-streaming platform working with independent content creators may wish to understand what drives users to engage with the platform’s content creators, so that engagement can increase for less-popular creators. As a starting point, the content creators with the most followers may have different characteristics that increase engagement versus less-popular creators. So, the streaming platform may wish to tune their dataset to determine if their recommendation system can generalize from more to less-popular creators.
- **Movie Recommender Systems = Common-Neighbors:** A movie-streaming platform wants to provide suggestions to users that are the most relevant to the user’s current interests. So, the movie platform sorts possible movie recommendations by how much overlap the movies share with one another. In order to enhance exposure to new movies that overlap with a user’s interests, the streaming platform can apply the Common Neighbor LPShift to their dataset to force the algorithm to generalize in a scenario where movies may not fully-overlap.

## B Heuristic Choice

Resource Allocation and Adamic-Adar Index were not considered for splitting strategies given that they build upon the original Common Neighbor formulation. Their inclusion is redundant given our intentions to induce distinctive structural shifts based on varying structural information, as described for each heuristic in Section 3.

## C Splitting Strategy – Additional Algorithmic Details

This section provides additional details about the way data was formatted before being used as input for Algorithm 1 of our proposed splitting strategy and the intuition behind how Preferential-Attachment and Shortest-Path work within the splitting strategy. The details on the algorithm includes:

- Validation and Testing Edges are limited to 100k edges total.
- PPA Training Edges are limited to 3 million edges total.
- Negative Testing and Validation edges are produced via HeART [31].
- Validation and testing edges that are duplicated with training edges are removed from the edge index.
- In order to provide overlap within a given dataset, validation and testing edges that do not connect to training nodes are removed from the edge index.
- After sampling the necessary training edges, the adjacency matrix is extracted from the edge index, converted to an undirected graph and has any edge weights standardized to 1.

Common Neighbors, Preferential-Attachment and Shortest-Path, as shown in Figure 2(a), 2(b), and 2(c) respectively, are interchangeable within the dataset splitting strategy. Details about how Common Neighbors functions within the strategy are included in Section 3.2. Figure 2(b) and Figure 2(c) serve as toy examples and do not correspond directly to any dataset splits tested within our study. However, the examples illustrated within Figure 2(b) and Figure 2(c) do correspond to how their given heuristic functions within our splitting strategy.

For Figure 2(b) or Preferential-Attachment, it determines the degrees between a given source and target node and then multiplies the two to produce the score, based on that score, the sample is then sorted into a new dataset split.

For Figure 2(c) or Shortest-Path, the heuristic determines the score by determining the minimum number of nodes necessary to reach the target node from the source node. If there is a link between the two nodes, we remove the link and then re-add to the adjacency matrix after the score calculation. The final Shortest-Path score applies the calculated shortest-path length,  $SP(u, v)$  as the denominator in a ratio of  $\frac{1}{SP(u, v)}$ , which is then used to sort the sample into its respective dataset split.

## D Additional Analysis Details

*Note:* We were unable to test CFLP [63] and EERM [54] after adapting their current implementations to our evaluation settings. CFLP experienced an out-of-memory error on all tested dataset splits. EERM experienced an out-of-memory error on every LPShift split of ogbl-ppa and exceeded 48 hours per run on ogbl-collab before converging.

The Holme-Kim graph used for analysis in Figure 7 was generated with the following parameters:

- $n = 235868$ ,  $m = 5$ ,  $p_c = 0.4$ , seed = 42

**Table 4: The cosine-similarity table of ogbl-collab’s original feature distribution and its LPShift versions.**

	Split	Train/Test	Train/Valid	Valid/Test
	Original	$83.50 \pm 7.33$	$83.40 \pm 7.33$	$86.91 \pm 6.58$
CN	(0,1,2)	$87.73 \pm 6.12$	$87.42 \pm 6.17$	$91.78 \pm 4.01$
	(0,2,4)	$87.06 \pm 6.08$	$86.72 \pm 6.14$	$91.01 \pm 4.29$
	(0,3,5)	$86.45 \pm 6.12$	$86.19 \pm 6.12$	$90.42 \pm 4.41$
	(2,1,0)	$85.53 \pm 6.74$	$85.22 \pm 6.79$	$90.45 \pm 4.49$
	(4,2,0)	$85.97 \pm 7.09$	$85.55 \pm 7.15$	$90.71 \pm 4.43$
	(5,3,0)	$86.08 \pm 7.29$	$85.62 \pm 7.34$	$90.74 \pm 4.53$
SP	( $\infty$ ,6,4)	$84.11 \pm 6.94$	$82.12 \pm 7.34$	$85.60 \pm 6.75$
	( $\infty$ ,4,3)	$84.35 \pm 6.93$	$82.66 \pm 7.45$	$85.97 \pm 6.75$
	(4,6, $\infty$ )	$81.10 \pm 7.74$	$82.15 \pm 7.79$	$81.86 \pm 7.48$
	(3,4, $\infty$ )	$81.99 \pm 7.84$	$82.81 \pm 7.98$	$82.76 \pm 7.72$
PA	(0,50,100)	$83.92 \pm 7.22$	$82.59 \pm 7.63$	$85.50 \pm 7.14$
	(0,100,200)	$87.48 \pm 6.16$	$87.55 \pm 6.10$	$92.52 \pm 3.70$
	(0,150,250)	$87.61 \pm 6.10$	$87.81 \pm 6.17$	$92.45 \pm 3.84$
	(100,50,0)	$82.28 \pm 7.96$	$83.22 \pm 8.00$	$83.17 \pm 7.85$
	(200,100,0)	$84.75 \pm 6.65$	$85.32 \pm 6.64$	$89.94 \pm 4.52$
	(250,150,0)	$85.08 \pm 6.65$	$85.51 \pm 6.64$	$90.62 \pm 4.46$

## E Time to Split Tested Dataset Samples

A key consideration for LPShift’s application as a splitting strategy is to alleviate the burden of gathering new datasets, allowing researchers to control for and then induce a distribution shift in link-prediction datasets quickly; without requiring an expensive and time-consuming project to build a new dataset. This consideration is inspired by current graph and node-classification benchmark datasets, all of which induce distribution shifts in pre-existing benchmark datasets [17],[22],[26]. LPShift is not meant to replace high-quality benchmark datasets, especially for distribution shifts, but to serve as a supplement for current datasets and enhance understanding of LP generalization. Results demonstrating LPShift’s time-efficiency on tested dataset splits are included below in Table 5.

**Table 5: The average time in seconds (s) across 10 runs to generate each ‘Forward’ and ‘Backward’ split for ogbl-ppa, ogbl-collab, ogbl-ddi.**

	Split	ogbl-collab	ogbl-ppa	ogbl-ddi
CN	(0, 1, 2)	7.48 s	177.89 s	13.45 s
	(0, 2, 4)	7.49 s	177.09 s	14.21 s
	(0, 3, 5)	7.63 s	178.23 s	13.64 s
	(2, 1, 0)	7.66 s	184.98 s	13.31 s
	(4, 2, 0)	7.63 s	186.49 s	13.71 s
	(5, 3, 0)	7.86 s	185.95 s	13.42 s
SP	( $\infty$ , 6, 4)	53.12 s	2748.64 s	–
	( $\infty$ , 4, 3)	52.24 s	2705.91 s	–
	(4, 6, $\infty$ )	53.93 s	2715.34 s	–
	(3, 4, $\infty$ )	53.7 s	2751.56 s	–
PA	(0, 50, 100)	19.25 s	406.5 s	15.41 s
	(0, 100, 200)	19.05 s	408.04 s	14.55 s
	(0, 150, 250)	19.35 s	407.81 s	13.96 s
	(100, 50, 0)	19.65 s	425.3 s	14.42 s
	(200, 100, 0)	19.34 s	409.93 s	14.59 s
	(250, 150, 0)	19.37 s	403.55 s	14.05 s



## F Size of Dataset Samples

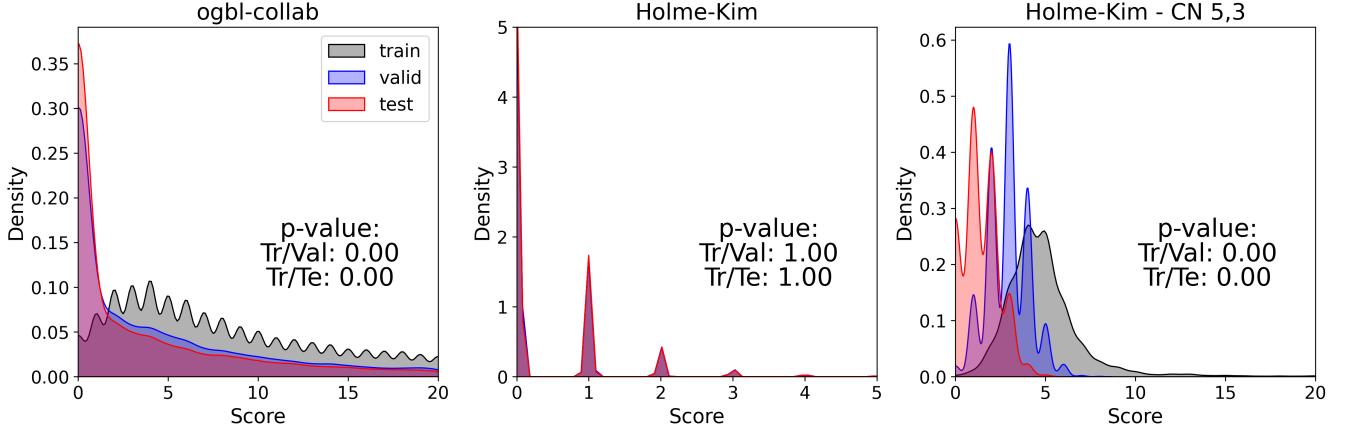
In this section we detail the number of training, validation, and test edges for all of the newly created splits detailed in Section 3. There are in Tables 6 for ogbl-collab, ogbl-ppa, and ogbl-ddi respectively.

Table 6: Number of samples in the ogbl-collab, ogbl-ppa, and ogbl-ddi datasets for the forward and backward heuristic splits, with shared split columns across datasets.

[illegible]

## G How effectively does LPShift induce distribution shift?

The following section will explore the capability of LPShift to induce a measurably-significant distribution shift in the structure of the ogbl-collab dataset. We apply the 2-sample Kolmogorov-Smirnov (KS) test [19] to compare if training, validation, and testing distributions can be sampled from one another, both before and after applying LPShift. As a controlled baseline to test LPShift, we generate a Holme-Kim (HK) graph [20] with a 40% chance to close a triangle, allowing the HK graph to contain numerous Common Neighbors without becoming fully-connected. HK graph generation parameters are included in Appendix D.



**Figure 7: Three subplots detailing CN distributions for: 1.) the unaltered ogbl-collab dataset 2.) a Holme-Kim (HK) graph with a random split 3.) the HK graph from 2. split with LPShift’s CN - 5,3 strategy**

The first subplot in Figure 7 extends the reasoning introduced with NCNC [48]. As such, this subplot indicates there is a natural shift for CNs within the original ogbl-collab dataset [21]. The p-value of 0, measured across both split permutations, indicates that the training distribution of CNs is shifted from the validation and testing distributions. The second subplot depicts a randomly-split HK graph [20], where CN distributions for each split match one another, further indicated by the p-values of 1. The third subplot depicts the HK graph from the second subplot split with LPShift’s CN - 5,3 strategy, resulting in a distinct shift between all dataset splits, as confirmed by the 0 p-values. As such, LPShift induces structural shift that is as measurably dissimilar as the structural shift present in the original ogbl-collab dataset, even when the initial dataset splits are measurably identical. Additionally, the CN - 5,3 split causes the shape of the HK graph’s CN distributions to become more similar to the shift observed within the original ogbl-collab dataset, indicating that the "Backward" LPShift strategy can function like a real-world distribution shift.

## H Dataset Results

In this section, we include all of the results for each experiment conducted on the LPShift dataset splits.

**Table 7: ogbl-collab results reported in MRR with the best bolded and the second best underlined.**

Split		Models						
		RA	GCN	BUDDY	NCNC	LPFormer	NeoGNN	SEAL
CN	(0, 1, 2)	<b>32.22</b>	$14.89 \pm 0.67$	<u><math>17.48 \pm 1.19</math></u>	$5.34 \pm 2.54$	$4.27 \pm 1.17$	$5.53 \pm 1.52$	$7.06 \pm 1.67$
	(0, 2, 4)	<b>29.74</b>	$17.75 \pm 0.44$	$15.47 \pm 0.57$	$13.99 \pm 1.35$	$12.97 \pm 1.24$	$13.26 \pm 0.39$	<u><math>20.60 \pm 6.23</math></u>
	(0, 3, 5)	<b>29.86</b>	$19.08 \pm 0.26$	$16.60 \pm 0.89$	$15.06 \pm 1.43$	<u><math>25.36 \pm 2.04</math></u>	$14.21 \pm 0.88$	$19.78 \pm 1.24$
	(2, 1, 0)	0.6	<b><math>5.04 \pm 0.13</math></b>	<u><math>3.70 \pm 0.13</math></u>	$1.46 \pm 0.02$	$2.01 \pm 0.95$	$2.16 \pm 0.05$	$1.01 \pm 0.02$
	(4, 2, 0)	4.79	<u><math>4.87 \pm 0.17</math></u>	$3.55 \pm 0.09$	<b><math>6.13 \pm 0.49</math></b>	$3.87 \pm 0.74$	$3.41 \pm 0.16$	$3.38 \pm 0.62$
	(5, 3, 0)	<b>15.9</b>	$6.78 \pm 0.19$	$5.40 \pm 0.04$	<u><math>12.87 \pm 1.50</math></u>	$8.36 \pm 0.63$	$7.85 \pm 0.74$	$8.08 \pm 1.96$
SP	( $\infty$ , 6, 4)	<b>33.87</b>	$12.64 \pm 0.85$	<u><math>16.20 \pm 1.40</math></u>	$14.43 \pm 1.36$	$4.6 \pm 3.15$	$6.14 \pm 1.44$	$2.08 \pm 1.50$
	( $\infty$ , 4, 3)	<b>33.91</b>	$15.50 \pm 0.16$	<u><math>16.42 \pm 2.30</math></u>	<u><math>18.33 \pm 1.24</math></u>	$15.7 \pm 2.87$	$5.82 \pm 1.20$	$2.10 \pm 1.24$
	(4, 6, $\infty$ )	0.69	<u><math>4.75 \pm 0.10</math></u>	<b><math>6.73 \pm 0.32</math></b>	$0.73 \pm 0.13$	$3.16 \pm 0.62$	$4.55 \pm 0.27$	$0.93 \pm 0.07$
	(3, 4, $\infty$ )	0.63	<b><math>3.81 \pm 0.16</math></b>	<u><math>3.71 \pm 0.39</math></u>	$0.95 \pm 0.24$	$1.86 \pm 0.48$	$2.54 \pm 0.09$	$0.80 \pm 0.01$
PA	(0, 50, 100)	<b>36.87</b>	$19.81 \pm 0.59$	$21.27 \pm 0.74$	$17.24 \pm 0.17$	$25.31 \pm 5.67$	$15.94 \pm 0.49$	<u><math>29.06 \pm 1.57</math></u>
	(0, 100, 200)	<b>26.78</b>	$12.68 \pm 0.20$	$14.04 \pm 0.76$	$12.34 \pm 3.01$	$11.98 \pm 3.12$	$13.50 \pm 0.84$	<u><math>20.69 \pm 1.51</math></u>
	(0, 150, 250)	<b>24.07</b>	$12.73 \pm 0.32$	$13.06 \pm 0.53$	$12.01 \pm 0.82$	$12.43 \pm 6.62$	$12.81 \pm 0.51$	<u><math>16.23 \pm 3.69</math></u>
	(100, 50, 0)	<b>33.09</b>	$24.33 \pm 0.537$	$24.95 \pm 0.92$	$20.81 \pm 1.86$	$17.76 \pm 2.01$	$6.42 \pm 0.462$	<u><math>31.83 \pm 6.44</math></u>
	(200, 100, 0)	<b>42.28</b>	$13.97 \pm 0.52$	$15.52 \pm 0.73$	$18.62 \pm 1.54$	$27.56 \pm 9.10$	$4.20 \pm 0.37$	<u><math>31.96 \pm 6.65</math></u>
	(250, 150, 0)	<b>44.14</b>	$12.98 \pm 0.45$	$13.36 \pm 0.83$	$18.71 \pm 0.99$	$24.04 \pm 11.35$	$4.40 \pm 0.63$	<u><math>39.58 \pm 4.81</math></u>

Table 8: ogbl-ppa results reported in MRR with the best bolded and the second best underlined.

Split		Models						
		RA	GCN	BUDDY	NCNC	LPFormer	NeoGNN	SEAL
CN	(0,1,2)	4.71	7.81 $\pm$ 0.08	<u>7.90 <math>\pm</math> 0.32</u>	7.08 $\pm$ 3.08	3.28 $\pm$ 0.63	3.49 $\pm$ 0.10	<b>11.91 <math>\pm</math> 1.85</b>
	(0,2,4)	4.45	<u>8.18 <math>\pm</math> 0.12</u>	3.83 $\pm$ 0.24	<b>9.89 <math>\pm</math> 1.92</b>	2.46 $\pm$ 0.51	5.79 $\pm$ 0.42	4.84 $\pm$ 0.10
	(0,3,5)	4.38	<b>8.75 <math>\pm</math> 0.19</b>	3.06 $\pm$ 0.06	<u>8.22 <math>\pm</math> 1.15</u>	4.84 $\pm$ 0.73	5.71 $\pm$ 0.26	5.15 $\pm$ 0.10
	(2,1,0)	0.53	<u>2.59 <math>\pm</math> 0.08</u>	1.60 $\pm$ 0.05	2.37 $\pm$ 0.15	<b>6.04 <math>\pm</math> 0.41</b>	0.76 $\pm$ 0.02	1.03 $\pm$ 0.54
	(4,2,0)	0.92	2.16 $\pm$ 0.05	2.47 $\pm$ 0.07	<b>8.54 <math>\pm</math> 0.74</b>	<u>4.23 <math>\pm</math> 0.46</u>	0.79 $\pm$ 0.00	0.95 $\pm$ 0.09
	(5,3,0)	1.17	2.17 $\pm$ 0.04	2.56 $\pm$ 0.08	<b>9.04 <math>\pm</math> 0.92</b>	<u>3.87 <math>\pm</math> 0.10</u>	0.86 $\pm$ 0.02	1.35 $\pm$ 0.56
SP	( $\infty$ ,6,4)	<b>32.57</b>	9.95 $\pm$ 0.52	1.24 $\pm$ 0.02	<u>11.16 <math>\pm</math> 8.81</u>	9.83 $\pm$ 5.92	3.13 $\pm$ 0.38	11.14 $\pm$ 12.06
	( $\infty$ ,4,3)	<b>19.84</b>	3.29 $\pm$ 0.10	<u>5.87 <math>\pm</math> 0.16</u>	0.79 $\pm$ 0.54	4.94 $\pm$ 0.62	3.58 $\pm$ 0.45	2.96 $\pm$ 4.58
	(4,6, $\infty$ )	0.65	<b>10.53 <math>\pm</math> 0.48</b>	<u>9.95 <math>\pm</math> 0.52</u>	5.84 $\pm$ 0.34	5.90 $\pm$ 1.76	4.89 $\pm$ 0.13	1.51 $\pm$ 0.72
	(3,4, $\infty$ )	0.54	<u>3.38 <math>\pm</math> 0.11</u>	<b>5.87 <math>\pm</math> 0.16</b>	1.01 $\pm$ 0.19	1.38 $\pm$ 0.46	0.83 $\pm$ 0.01	0.51 $\pm$ 0.02
PA	(0,5k,10k)	3.9	3.69 $\pm$ 0.76	3.93 $\pm$ 0.98	<u>8.00 <math>\pm</math> 0.60</u>	<b>9.27 <math>\pm</math> 1.78</b>	4.92 $\pm$ 0.58	4.22 $\pm$ 0.63
	(0,10k,20k)	3.14	3.42 $\pm$ 0.59	6.38 $\pm$ 3.48	<u>6.90 <math>\pm</math> 1.46</u>	<b>9.03 <math>\pm</math> 1.6</b>	6.29 $\pm$ 0.87	3.43 $\pm$ 0.19
	(0,15k,25k)	2.72	5.62 $\pm$ 0.40	2.48 $\pm$ 0.03	8.00 $\pm$ 0.78	<b>9.07 <math>\pm</math> 2.43</b>	<u>8.98 <math>\pm</math> 1.10</u>	3.57 $\pm$ 0.74
	(10k,5k,0)	7.4	3.09 $\pm$ 0.15	3.15 $\pm$ 0.16	<u>10.56 <math>\pm</math> 0.73</u>	<b>14.43 <math>\pm</math> 4.45</b>	1.52 $\pm$ 0.05	4.88 $\pm$ 0.90
	(20k,10k,0)	5.81	2.50 $\pm$ 0.23	2.55 $\pm$ 0.16	<u>7.74 <math>\pm</math> 0.46</u>	<b>8.43 <math>\pm</math> 3.46</b>	1.38 $\pm$ 0.04	4.50 $\pm$ 1.10
	(25k,15k,0)	5.08	2.79 $\pm$ 0.28	2.37 $\pm$ 0.02	<u>7.82 <math>\pm</math> 0.36</u>	<b>6.27 <math>\pm</math> 3.87</b>	1.39 $\pm$ 0.06	2.38 $\pm$ 0.73

Table 9: ogbl-ddi results reported in MRR with the best bolded and the second best underlined.

Split		Models						
		RA	GCN	BUDDY	NCNC	LPFormer	NeoGNN	SEAL
CN	(0,1,2)	<u>4.8</u>	<b>5.34 <math>\pm</math> 0.24</b>	1.65 $\pm$ 0.17	0.79 $\pm$ 0.20	0.82 $\pm$ 0.21	0.92 $\pm$ 0.01	0.89 $\pm$ 0.39
	(0,2,4)	<u>4.25</u>	<b>4.88 <math>\pm</math> 0.41</b>	2.75 $\pm$ 0.16	1.39 $\pm$ 0.81	0.85 $\pm$ 0.14	2.12 $\pm$ 0.77	1.17 $\pm$ 0.32
	(0,3,5)	<b>3.86</b>	<u>3.48 <math>\pm</math> 0.26</u>	2.15 $\pm$ 0.08	1.88 $\pm$ 0.57	1.06 $\pm$ 0.17	1.75 $\pm$ 0.44	0.98 $\pm$ 0.37
	(2,1,0)	0.46	1.14 $\pm$ 0.20	0.78 $\pm$ 0.06	<u>2.05 <math>\pm</math> 2.58</u>	<b>3.13 <math>\pm</math> 0.63</b>	0.94 $\pm$ 0.40	0.87 $\pm$ 0.49
	(4,2,0)	0.59	1.01 $\pm$ 0.20	1.09 $\pm$ 0.22	0.61 $\pm$ 0.17	<b>3.46 <math>\pm</math> 0.61</b>	<u>2.66 <math>\pm</math> 1.94</u>	0.62 $\pm$ 0.08
	(5,3,0)	0.54	1.41 $\pm$ 0.32	1.40 $\pm$ 0.35	0.58 $\pm$ 0.03	<b>3.94 <math>\pm</math> 0.28</b>	<u>2.69 <math>\pm</math> 1.89</u>	0.62 $\pm$ 0.07
PA	(0,5k,10k)	<b>5.29</b>	2.61 $\pm$ 0.38	1.81 $\pm$ 0.35	<u>3.44 <math>\pm</math> 1.73</u>	1.19 $\pm$ 0.11	1.96 $\pm$ 0.72	0.83 $\pm$ 0.30
	(0,10k,20k)	<b>3.6</b>	1.96 $\pm$ 0.22	1.74 $\pm$ 0.28	<u>2.70 <math>\pm</math> 0.53</u>	0.84 $\pm$ 0.21	1.31 $\pm$ 0.30	1.35 $\pm$ 0.87
	(0,15k,25k)	<b>2.54</b>	1.91 $\pm$ 0.14	1.92 $\pm$ 0.08	<u>2.33 <math>\pm</math> 1.18</u>	1.46 $\pm$ 0.31	1.31 $\pm$ 0.20	1.48 $\pm$ 0.69
	(10k,5k,0)	7.06	4.68 $\pm$ 1.19	1.19 $\pm$ 0.32	<u>12.55 <math>\pm</math> 15.18</u>	<b>14.19 <math>\pm</math> 5.59</b>	3.63 $\pm$ 0.50	4.64 $\pm$ 4.21
	(20k,10k,0)	1.5	2.04 $\pm$ 0.77	2.71 $\pm$ 1.60	<b>10.03 <math>\pm</math> 9.20</b>	<u>8.26 <math>\pm</math> 1.13</u>	2.89 $\pm$ 0.81	1.31 $\pm$ 0.92
	(25k,15k,0)	1.68	1.14 $\pm$ 0.39	2.09 $\pm$ 0.72	<u>4.66 <math>\pm</math> 4.89</u>	<b>8.51 <math>\pm</math> 0.82</b>	1.58 $\pm$ 0.98	1.71 $\pm$ 0.56

**Table 10: ogbl-collab results on the forward and backward splits. Results are reported for DropEdge and TC (BUDDY) and for GCN+BUDDY and RA+BUDDY (Filter+Rank).**

Split	BUDDY		Filter+Rank		
	DropEdge	TC	GCN+BUDDY	RA+BUDDY	
CN	(0, 1, 2)	15.54 ± 0.98	11.27 ± 2.03	8.50 ± 1.10	3.94 ± 0.51
	(0, 2, 4)	16.16 ± 0.17	12.39 ± 1.43	12.85 ± 0.83	6.61 ± 0.30
	(0, 3, 5)	16.34 ± 0.17	14.99 ± 1.69	15.35 ± 0.96	7.16 ± 0.09
	(2, 1, 0)	2.61 ± 0.09	5.28 ± 0.05	5.46 ± 0.11	4.32 ± 0.19
	(4, 2, 0)	2.88 ± 0.11	5.23 ± 0.05	5.36 ± 0.12	4.45 ± 0.12
	(5, 3, 0)	4.99 ± 0.08	6.03 ± 0.10	5.96 ± 0.06	4.93 ± 0.11
	SP	(∞, 6, 4)	12.31 ± 0.51	7.25 ± 0.81	7.38 ± 0.82
(∞, 4, 3)		17.11 ± 1.02	9.33 ± 1.66	9.60 ± 0.39	7.63 ± 0.25
(4, 6, ∞)		5.34 ± 0.43	6.88 ± 0.30	6.86 ± 1.13	6.86 ± 1.13
(3, 4, ∞)		2.93 ± 0.18	6.24 ± 0.13	6.47 ± 0.24	6.47 ± 0.24
PA	(0, 50, 100)	21.35 ± 0.36	18.82 ± 1.35	15.92 ± 1.01	15.92 ± 1.01
	(0, 100, 200)	13.84 ± 0.64	12.13 ± 1.04	9.47 ± 0.31	9.47 ± 0.31
	(0, 150, 250)	12.85 ± 0.78	10.63 ± 0.55	9.60 ± 0.41	9.60 ± 0.41
	(100, 50, 0)	26.09 ± 0.62	15.84 ± 1.13	14.34 ± 1.05	14.34 ± 1.05
	(200, 100, 0)	15.68 ± 0.85	9.15 ± 0.39	8.35 ± 0.34	8.35 ± 0.34
	(250, 150, 0)	13.13 ± 0.94	6.70 ± 0.20	5.50 ± 0.33	5.50 ± 0.33



**Table 11: ogbl-ppa results on the forward and backward splits. Results are reported for DropEdge and TC (BUDDY) and for GCN+BUDDY and RA+BUDDY (Filter+Rank).**

Split		BUDDY		Filter+Rank	
		DropEdge	TC	GCN+BUDDY	RA+BUDDY
CN	(0, 1, 2)	$7.83 \pm 0.27$	$5.27 \pm 0.34$	$4.48 \pm 0.33$	$4.04 \pm 0.26$
	(0, 2, 4)	$3.83 \pm 0.25$	$2.91 \pm 0.06$	$3.79 \pm 0.28$	$3.42 \pm 0.20$
	(0, 3, 5)	$3.06 \pm 0.06$	$2.67 \pm 0.13$	$3.16 \pm 0.10$	$2.95 \pm 0.13$
	(2, 1, 0)	$1.61 \pm 0.04$	$3.44 \pm 0.08$	$3.19 \pm 0.08$	$2.58 \pm 0.09$
	(4, 2, 0)	$2.47 \pm 0.07$	$3.45 \pm 0.10$	$3.25 \pm 0.09$	$3.04 \pm 0.05$
	(5, 3, 0)	$2.56 \pm 0.08$	$3.55 \pm 0.13$	$3.36 \pm 0.13$	$3.10 \pm 0.15$
SP	( $\infty$ , 6, 4)	$3.86 \pm 0.39$	$4.00 \pm 0.29$	$4.00 \pm 0.20$	$3.89 \pm 0.23$
	( $\infty$ , 4, 3)	$5.87 \pm 0.16$	$4.82 \pm 0.39$	$5.53 \pm 0.92$	$5.53 \pm 0.94$
	(4, 6, $\infty$ )	$3.86 \pm 0.39$	$13.2 \pm 0.45$	$14.41 \pm 0.67$	$13.63 \pm 0.97$
	(3, 4, $\infty$ )	$5.87 \pm 0.16$	$2.89 \pm 0.09$	$2.93 \pm 0.15$	$2.51 \pm 0.14$
PA	(0, 5k, 10k)	$3.93 \pm 0.98$	$3.62 \pm 0.21$	$3.66 \pm 0.38$	$3.66 \pm 0.38$
	(0, 10k, 20k)	$6.38 \pm 3.48$	$3.13 \pm 0.12$	$3.19 \pm 0.22$	$3.19 \pm 0.22$
	(0, 15k, 25k)	$2.49 \pm 0.01$	$3.33 \pm 1.38$	$2.88 \pm 0.06$	$2.88 \pm 0.06$
	(10k, 5k, 0)	$3.13 \pm 0.10$	$1.78 \pm 0.16$	$2.05 \pm 0.05$	$2.05 \pm 0.04$
	(20k, 10k, 0)	$2.56 \pm 0.19$	$1.50 \pm 0.0008$	$1.67 \pm 0.03$	$1.65 \pm 0.05$
	(25k, 15k, 0)	$2.40 \pm 0.03$	$1.53 \pm 0.04$	$1.66 \pm 0.02$	$1.64 \pm 0.03$

**Table 12: ogbl-ddi results on the forward and backward splits. Results are reported for DropEdge and TC (BUDDY) and for GCN+BUDDY and RA+BUDDY (Filter+Rank).**

Split		BUDDY		Filter+Rank	
		DropEdge	TC	GCN+BUDDY	RA+BUDDY
CN	(0, 1, 2)	$1.65 \pm 0.17$	$1.1 \pm 0.01$	$0.87 \pm 0.21$	$0.87 \pm 0.21$
	(0, 2, 4)	$2.75 \pm 0.16$	$1.01 \pm 0.01$	$1.45 \pm 0.35$	$1.45 \pm 0.35$
	(0, 3, 5)	$2.15 \pm 0.08$	$0.94 \pm 0.01$	$1.65 \pm 0.22$	$1.65 \pm 0.22$
	(2, 1, 0)	$0.78 \pm 0.06$	$1.04 \pm 0.02$	$1.20 \pm 0.14$	$1.20 \pm 0.14$
	(4, 2, 0)	$1.09 \pm 0.22$	$0.9 \pm 0.02$	$2.44 \pm 0.27$	$2.44 \pm 0.27$
	(5, 3, 0)	$1.40 \pm 0.35$	$0.98 \pm 0.03$	$3.19 \pm 0.36$	$3.19 \pm 0.36$
PA	(0, 5k, 10k)	$1.81 \pm 0.35$	$1.04 \pm 0.01$	$1.26 \pm 0.28$	$1.26 \pm 0.28$
	(0, 10k, 20k)	$1.74 \pm 0.28$	$1.06 \pm 0.02$	$1.43 \pm 0.1$	$1.43 \pm 0.11$
	(0, 15k, 25k)	$1.92 \pm 0.08$	$1.24 \pm 0.02$	$1.04 \pm 0.23$	$1.04 \pm 0.23$
	(10k, 5k, 0)	$3.83 \pm 3.22$	$1.0 \pm 0.03$	$9.16 \pm 9.27$	$9.16 \pm 9.27$
	(20k, 10k, 0)	$2.71 \pm 1.60$	$1.66 \pm 0.01$	$9.84 \pm 1.97$	$9.84 \pm 1.97$
	(25k, 15k, 0)	$11.07 \pm 1.44$	$1.95 \pm 0.02$	$9.50 \pm 2.18$	$9.50 \pm 2.18$

**Table 13: MRR Results for traditional generalization methods applied to GCN on the Forward splits for ogbl-collab. Generalization methods that significantly improve performance are bolded.**

Models	CN Splits			SP Splits		PA Splits		
	(0, 1, 2)	(0, 2, 4)	(0, 3, 5)	( $\infty$ , 6, 4)	( $\infty$ , 4, 3)	(0, 50, 100)	(0, 100, 200)	(0, 150, 250)
GCN	14.89 $\pm$ 0.67	17.75 $\pm$ 0.44	19.08 $\pm$ 0.26	12.64 $\pm$ 0.85	15.50 $\pm$ 0.16	19.81 $\pm$ 0.59	12.68 $\pm$ 0.20	12.73 $\pm$ 0.32
+IRM	7.40 $\pm$ 0.32	6.97 $\pm$ 0.55	5.50 $\pm$ 0.71	5.84 $\pm$ 0.58	5.28 $\pm$ 0.17	11.18 $\pm$ 1.46	6.88 $\pm$ 1.65	6.95 $\pm$ 1.09
+VREx	14.31 $\pm$ 0.76	16.95 $\pm$ 0.22	18.86 $\pm$ 0.13	13.17 $\pm$ 0.58	15.75 $\pm$ 0.50	21.69 $\pm$ 0.18	15.23 $\pm$ 0.44	14.66 $\pm$ 0.14
+GroupDRO	5.13 $\pm$ 0.55	5.19 $\pm$ 0.61	5.51 $\pm$ 0.67	6.27 $\pm$ 0.91	6.36 $\pm$ 0.53	9.56 $\pm$ 1.93	7.39 $\pm$ 0.65	6.04 $\pm$ 0.90
+DANN	15.69 $\pm$ 0.28	16.83 $\pm$ 0.18	18.80 $\pm$ 0.20	14.01 $\pm$ 0.37	15.60 $\pm$ 0.45	21.77 $\pm$ 0.31	15.61 $\pm$ 0.30	14.89 $\pm$ 0.11
+Deep CORAL	14.31 $\pm$ 0.76	16.95 $\pm$ 0.22	18.84 $\pm$ 0.10	13.26 $\pm$ 0.68	15.60 $\pm$ 0.29	21.69 $\pm$ 0.18	15.00 $\pm$ 0.28	14.59 $\pm$ 0.13
	(2, 1, 0)	(4, 2, 0)	(5, 3, 0)	(4, 6, $\infty$ )	(3, 4, $\infty$ )	(100, 50, 0)	(200, 100, 0)	(250, 150, 0)
GCN	5.04 $\pm$ 0.13	4.87 $\pm$ 0.17	6.78 $\pm$ 0.19	4.75 $\pm$ 0.10	3.81 $\pm$ 0.16	24.33 $\pm$ 0.53	13.97 $\pm$ 0.52	12.98 $\pm$ 0.45
+IRM	2.42 $\pm$ 0.28	3.21 $\pm$ 0.29	3.08 $\pm$ 0.41	2.39 $\pm$ 0.37	1.81 $\pm$ 1.11	2.72 $\pm$ 1.12	2.00 $\pm$ 0.90	1.99 $\pm$ 0.70
+VREx	5.10 $\pm$ 0.04	5.60 $\pm$ 0.25	6.91 $\pm$ 0.15	4.67 $\pm$ 0.08	3.92 $\pm$ 0.22	23.06 $\pm$ 0.59	12.53 $\pm$ 0.21	11.81 $\pm$ 0.31
+GroupDRO	3.38 $\pm$ 0.26	2.77 $\pm$ 0.07	2.99 $\pm$ 0.02	3.04 $\pm$ 0.75	2.88 $\pm$ 0.74	3.49 $\pm$ 0.64	3.32 $\pm$ 0.42	3.49 $\pm$ 0.92
+DANN	5.47 $\pm$ 0.11	5.40 $\pm$ 0.25	6.98 $\pm$ 0.28	8.63 $\pm$ 0.32	6.65 $\pm$ 0.52	21.83 $\pm$ 0.61	12.53 $\pm$ 0.46	11.67 $\pm$ 0.22
+Deep CORAL	5.13 $\pm$ 0.08	5.49 $\pm$ 0.13	6.82 $\pm$ 0.13	8.47 $\pm$ 0.18	6.72 $\pm$ 0.36	23.10 $\pm$ 0.67	12.52 $\pm$ 0.20	11.80 $\pm$ 0.31

**Table 14: MRR Results for traditional generalization methods applied to GCN on the Forward splits for ogbl-ppa. Generalization methods that significantly improve performance are bolded.**

Models	CN Splits			SP Splits		PA Splits		
	(0, 1, 2)	(0, 2, 4)	(0, 3, 5)	( $\infty$ , 6, 4)	( $\infty$ , 4, 3)	(0, 5k, 10k)	(0, 10k, 20k)	(0, 15k, 25k)
GCN	7.81 $\pm$ 0.08	8.18 $\pm$ 0.12	8.75 $\pm$ 0.19	6.34 $\pm$ 0.72	5.05 $\pm$ 0.08	3.69 $\pm$ 0.76	3.42 $\pm$ 0.59	5.62 $\pm$ 0.40
+IRM	1.99 $\pm$ 0.45	1.97 $\pm$ 1.37	2.30 $\pm$ 1.05	6.44 $\pm$ 0.62	4.98 $\pm$ 0.15	3.01 $\pm$ 0.61	5.24 $\pm$ 0.20	3.13 $\pm$ 0.56
+VREx	6.91 $\pm$ 0.18	7.32 $\pm$ 0.25	7.81 $\pm$ 0.21	6.35 $\pm$ 0.83	5.19 $\pm$ 0.23	4.30 $\pm$ 0.77	3.94 $\pm$ 0.83	4.71 $\pm$ 0.85
+GroupDRO	2.34 $\pm$ 0.19	2.31 $\pm$ 0.27	2.52 $\pm$ 0.37	5.03 $\pm$ 1.91	2.62 $\pm$ 1.03	3.06 $\pm$ 0.44	4.70 $\pm$ 0.60	2.77 $\pm$ 0.32
+DANN	7.06 $\pm$ 0.19	7.34 $\pm$ 0.14	7.82 $\pm$ 0.18	6.34 $\pm$ 1.05	5.30 $\pm$ 0.38	4.28 $\pm$ 0.87	4.74 $\pm$ 1.12	5.66 $\pm$ 0.36
+Deep CORAL	6.91 $\pm$ 0.18	7.32 $\pm$ 0.25	7.79 $\pm$ 0.22	6.25 $\pm$ 0.62	5.18 $\pm$ 0.23	4.19 $\pm$ 0.76	4.08 $\pm$ 0.73	4.57 $\pm$ 0.74
	(2, 1, 0)	(4, 2, 0)	(5, 3, 0)	(4, 6, $\infty$ )	(3, 4, $\infty$ )	(10k, 5k, 0)	(20k, 10k, 0)	(25k, 15k, 0)
GCN	2.59 $\pm$ 0.08	2.16 $\pm$ 0.05	2.17 $\pm$ 0.04	9.95 $\pm$ 0.52	3.29 $\pm$ 0.10	3.09 $\pm$ 0.15	2.50 $\pm$ 0.23	2.79 $\pm$ 0.28
+IRM	1.78 $\pm$ 0.56	3.05 $\pm$ 0.17	3.00 $\pm$ 0.32	2.34 $\pm$ 2.07	1.88 $\pm$ 0.64	3.98 $\pm$ 0.23	3.21 $\pm$ 0.28	3.09 $\pm$ 0.12
+VREx	3.51 $\pm$ 0.28	2.91 $\pm$ 0.11	2.87 $\pm$ 0.17	9.42 $\pm$ 0.85	3.48 $\pm$ 0.32	3.41 $\pm$ 0.86	2.50 $\pm$ 0.48	2.57 $\pm$ 0.49
+GroupDRO	1.85 $\pm$ 0.42	3.20 $\pm$ 0.23	3.23 $\pm$ 0.16	2.19 $\pm$ 0.29	2.09 $\pm$ 0.60	4.42 $\pm$ 0.26	3.37 $\pm$ 0.08	3.07 $\pm$ 0.13
+DANN	3.62 $\pm$ 0.29	2.72 $\pm$ 0.18	2.73 $\pm$ 0.11	9.69 $\pm$ 0.46	3.32 $\pm$ 0.07	2.71 $\pm$ 0.25	2.13 $\pm$ 0.18	2.20 $\pm$ 0.20
+Deep CORAL	3.43 $\pm$ 0.34	2.93 $\pm$ 0.11	2.70 $\pm$ 0.08	9.42 $\pm$ 0.85	3.48 $\pm$ 0.32	2.57 $\pm$ 0.45	2.13 $\pm$ 0.36	2.14 $\pm$ 0.15

**Table 15: MRR Results for traditional generalization methods applied to GCN on the Forward splits for ogbl-ddi. Generalization methods that significantly improve performance are bolded.**

Models	CN Splits			PA Splits		
	(0, 1, 2)	(0, 2, 4)	(0, 3, 5)	(0, 5k, 10k)	(0, 10k, 20k)	(0, 15k, 25k)
GCN	5.34 $\pm$ 0.24	4.88 $\pm$ 0.41	3.48 $\pm$ 0.26	2.61 $\pm$ 0.38	1.96 $\pm$ 0.22	1.91 $\pm$ 0.14
+IRM	0.77 $\pm$ 0.16	1.36 $\pm$ 0.46	1.26 $\pm$ 0.19	1.34 $\pm$ 0.43	1.55 $\pm$ 0.57	1.90 $\pm$ 1.17
+VREx	0.64 $\pm$ 0.02	0.61 $\pm$ 0.02	1.41 $\pm$ 0.43	2.09 $\pm$ 0.29	1.28 $\pm$ 0.71	1.13 $\pm$ 0.21
+GroupDRO	0.64 $\pm$ 0.02	1.89 $\pm$ 0.72	0.77 $\pm$ 0.16	1.12 $\pm$ 0.14	0.84 $\pm$ 0.22	2.22 $\pm$ 1.11
+DANN	0.63 $\pm$ 0.02	0.98 $\pm$ 0.82	1.44 $\pm$ 0.50	2.19 $\pm$ 0.16	1.12 $\pm$ 0.54	1.19 $\pm$ 0.20
+Deep CORAL	0.64 $\pm$ 0.02	0.61 $\pm$ 0.02	1.29 $\pm$ 0.30	2.22 $\pm$ 0.44	1.23 $\pm$ 0.72	1.16 $\pm$ 0.20
	(2, 1, 0)	(4, 2, 0)	(5, 3, 0)	(10k, 5k, 0)	(20k, 10k, 0)	(25k, 15k, 0)
GCN	1.14 $\pm$ 0.20	1.01 $\pm$ 0.20	1.41 $\pm$ 0.32	4.68 $\pm$ 1.19	2.04 $\pm$ 0.77	1.14 $\pm$ 0.39
+IRM	4.32 $\pm$ 0.64	4.03 $\pm$ 1.02	4.94 $\pm$ 2.16	5.22 $\pm$ 2.91	5.69 $\pm$ 2.68	6.74 $\pm$ 0.85
+VREx	4.08 $\pm$ 0.63	3.63 $\pm$ 0.01	4.14 $\pm$ 0.97	3.67 $\pm$ 1.76	2.61 $\pm$ 2.36	6.27 $\pm$ 0.58
+GroupDRO	4.58 $\pm$ 1.33	3.68 $\pm$ 0.31	3.62 $\pm$ 0.01	4.13 $\pm$ 3.55	3.05 $\pm$ 3.23	6.37 $\pm$ 0.03
+DANN	4.91 $\pm$ 1.31	3.66 $\pm$ 0.10	4.78 $\pm$ 1.48	4.11 $\pm$ 2.44	2.22 $\pm$ 2.03	6.29 $\pm$ 1.32
+Deep CORAL	4.08 $\pm$ 0.63	3.63 $\pm$ 0.01	4.06 $\pm$ 1.00	3.51 $\pm$ 1.63	1.71 $\pm$ 1.71	6.19 $\pm$ 0.59

## I Earth Mover's Distance (EMD) Results

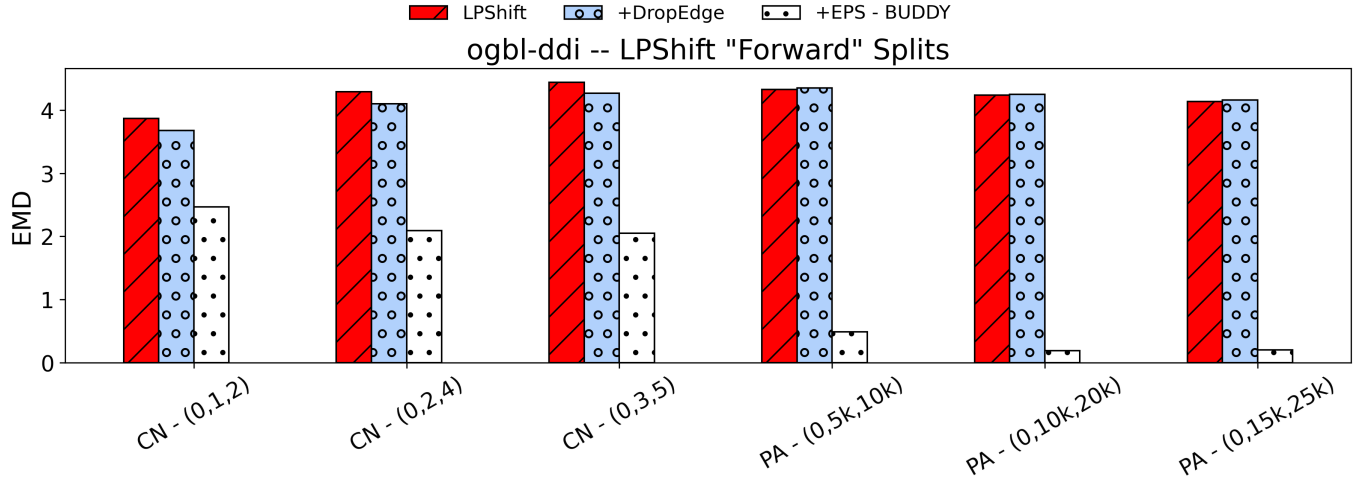


Figure 8: The EMD values calculated between the heuristic scores of training and testing samples on the "Backward" LPShift splits before and after applying structural generalization methods. *Note:* The tested heuristics correspond to their labelled LPShift splits, so as to simulate the dataset splitting.

Table 16: EMD calculations for ogbl-collab, ogbl-ppa, and ogbl-ddi on the forward and backward splits. (Note: Scores with a distance multiple-times different than the baseline are in bold for ogbl-collab.)

Split	ogbl-collab			ogbl-ppa			ogbl-ddi			
	Baseline	DropEdge	EPS	Baseline	DropEdge	EPS	Baseline	DropEdge	EPS	
CN	(0, 1, 2)	1.31	1.31	<b>3.6</b>	2.82	2.82	>24hrs	3.87	3.68	2.47
	(0, 2, 4)	1.6	1.6	2.52	3.13	3.13	>24hrs	4.29	4.1	2.09
	(0, 3, 5)	1.45	1.65	2.22	3.05	3.19	>24hrs	4.44	4.27	2.05
	(2, 1, 0)	1.87	1.15	2.91	3.1	2.36	>24hrs	5.81	5.62	4.1
	(4, 2, 0)	2.26	1.49	2.99	3.3	2.55	>24hrs	5.81	5.62	4.17
	(5, 3, 0)	2.28	1.52	2.14	3.19	2.44	>24hrs	5.69	5.44	4.08
SP	( $\infty$ , 6, 4)	5.93	5.94	<b>0.012</b>	5.81	5.84	>24hrs	–	–	–
	( $\infty$ , 4, 3)	5.35	5.38	<b>0.003</b>	1.36	1.4	>24hrs	–	–	–
	(4, 6, $\infty$ )	3.6	3.53	<b>1.22</b>	2.14	2.14	>24hrs	–	–	–
	(3, 4, $\infty$ )	1.85	1.78	3.23	0.72	0.72	>24hrs	–	–	–
PA	(0, 50, 100)	1.87	1.89	3.42	2.55	2.55	>24hrs	4.33	4.35	<b>0.49</b>
	(0, 100, 200)	2.29	2.32	2.72	2.76	2.76	>24hrs	4.24	4.25	<b>0.19</b>
	(0, 150, 250)	2.34	2.36	3.08	2.78	2.78	>24hrs	4.14	4.16	<b>0.20</b>
	(100, 50, 0)	4.29	4.3	2.48	2.96	2.96	>24hrs	6.85	6.92	<b>0.71</b>
	(200, 100, 0)	3.79	3.82	<b>0.78</b>	2.68	2.68	>24hrs	6.41	6.49	<b>0.58</b>
	(250, 150, 0)	3.48	3.5	2.48	2.48	2.48	>24hrs	5.98	6.02	<b>0.44</b>

## J Additional Training Details

This section provides relevant details about training and reproducing results not mentioned in Section 5.1:

Please consult the project README for building the project, loading data, and re-creating results. Tuned model hyperparameters are further detailed within their respective run scripts.

**Table 17: Fixed Model Hyperparameters by model. *Note:* Hidden channels were fixed across all datasets.**

	GCN	BUDDY	NCNC	NeoGNN	LPFormer	SEAL
Hidden Channels	128	256	256	256	128	256

- All models and link predictors are each fixed to 3 layers in their neural architecture.
- All experiments were conducted with a single A6000 48GB GPU and 1TB of available system RAM.
- We apply the 'NCNC2' variant of NCNC with an added depth argument of 2 [48] for all CN and SP splits of ogbl-collab. Otherwise, we set depth equal to 1, so as to reduce runtime.
- NeoGNN use 1-hop neighborhoods on all tested datasets.
- The learning rate and dropout for batch size tuning was fixed at  $1e^{-3}$  and 0.1 respectively. The model performance and memory complexity was tested in single runs with the following batch sizes: {8, 16, 32, 64, 128, 256, 512, 1024, 2048, 4096, 8192, 16384, 32768, 65536}.

## K Dataset Licenses

The dataset splitting strategy proposed in this paper is built using Pytorch Geometric (PyG). As such, this project's software and the PyG datasets are freely-available under the MIT license.

## L Limitations

The proposed dataset splitting strategy is restricted to inducing distribution shifts solely with neighborhood heuristics on static graphs. So, it does not directly consider other types of possible distribution shifts for the link prediction task (i.e. spatio-temporal [62] or size [67] shift). Additionally, since the neighborhood heuristics compute discrete scores produced from an input graph's structural information and effectively training GNN4LP models requires no leakage with validation/testing, it may be difficult to determine the correct thresholds to extract a meaningful number of samples. For Common Neighbors and Preferential-Attachment, this is especially relevant with smaller training graphs, given that larger and/or denser graphs have inherently more edges. Therefore, larger and denser graphs have inherently more possible Common Neighbors and Preferential-Attachment scores. For Shortest-Path, splitting can be exceptionally difficult for denser graphs, as demonstrated with the tiny split sizes for ogbl-ppa in Table 6.

## M Impact Statement

Our proposed dataset splitting strategy mimics the formatting of PyTorch Geometric datasets. This means that our strategy is simple to implement, enabling future work involved with understanding this type of structural shift for link prediction and promoting beginner-friendly practices for artificial intelligence research. Additionally, since the structural shift we propose in this article affects real-life systems, which integrate link prediction models, this research can provide a foundation for the improvement of relevant technologies; which holds positive ramifications for society and future research. No apparent risk is related to the contribution of this work.